Frictional Properties of Automatic Transmission Fluids: Part 2: Origins of Friction-Sliding Speed Behaviour

M. Ingram[1], J. Noles[2], R. Watts[2], S.Harris,[3]. H. A. Spikes[1]
[1] Tribology Group, Department of Mechanical Engineering, Imperial College London, UK, SW7 2AZ
[2] Infineum USA LP, Linden, New Jersey, USA
[3] Infineum UK Ltd, Milton Hill, Abingdon, UK

1. INTRODUCTION

A wet clutch consists of a series of alternating friction material and steel separator discs immersed in transmission fluid and its effective performance depends on the friction between these pairs of discs. In order to engage and disengage efficiently, this friction must be high, but in order to prevent noisy and uncomfortable stick-slip effects, it should also increase with sliding speed. Such friction-speed behaviour is atypical, since in most liquid lubricated, sliding systems friction decreases as sliding speed is raised. This is because faster sliding leads to more lubricant entrainment, so that the contact moves from high friction boundary to low friction fluid film lubrication. There has been considerable debate as to how it is possible for friction to increase with sliding speed in a wet clutch contact.

The companion paper, Part 1, described the development and use of a simple bench test to measure friction *versus* sliding speed characteristics of friction material rubbing against steel, lubricated with a range of fluids. The results showed the impact of lubricant additives on the friction behaviour and demonstrated how the addition of organic friction modifiers leads to the characteristic behaviour of friction that increases with speed.

This paper, Part 2, discusses possible mechanisms for the observed friction behaviour and, in particular, for the underlying mechanism that enables friction to increase with increase of sliding speed in a wet clutch contact.

The paper is in four sections. In the first it is shown, based on previous and new work, that a full, separating hydrodynamic film is never established within a sliding wet clutch contact. This is because of the very rough, fibre-based topography of the friction material coupled with its porosity, which means that the real contact comprises a very small fraction of the apparent contact area and consists of tiny, independent, load bearing “contact units”. From measurements of the real contact area and the number of contact units, the local geometry and conditions of these contact units can be determined.

In the second section, the various suggestions made in the literature to explain why friction increases with speed in a sliding wet clutch are listed and discussed.

A new hypothesis is proposed by the authors in the third section of the paper. This is that an increase in friction with sliding speed is an inherent property of “effective”, organic boundary lubricating films. This new hypothesis is then developed to explain how some additives increase friction at high speeds in a wet clutch.

Finally, in the fourth section of the paper, the origin of the friction rise at low sliding speeds seen for base oil and formulations that do not contain effective organic friction modifiers is considered and a new mechanism based on capillary forces is proposed for this behaviour.

2. CONTACT UNIT MODEL OF WET CLUTCH CONTACT

There has been considerable previous research to elucidate the regime of lubrication in wet clutches. A popular approach has been to measure friction in an LVFA over a wide range of bearing index values *S*, obtained by using different sliding speeds and lubricant viscosities. According to hydrodynamic lubrication theory, the bearing index, defined as $S = u_s \eta / p_{mean}$, controls the extent of fluid entrainment within sliding contacts and thus the hydrodynamic film thickness (Stachowiak and Batchelor *(1)*). This parameter is equivalent to that used to portray friction curves such as the well known Stribeck curve. However, for friction material/steel contacts, it has been found that friction remains high in the range 0.1 to 0.2 even at high bearing index values. This suggests that full hydrodynamic lubrication, in which most or all the applied load is supported by a pressurised fluid film, is never achieved in such contacts (Sano and Takesue *(2)*; Matsumoto *(3)*; Ito *et al. (4)*; Miyazaki and Hoshino *(5)*). This was confirmed in the current study, where the sliding MTM sliding friction test method described in Part I was used to measure friction at medium to high speeds (0.01m/s to 5 m/s) using a high viscosity polyalphaolfin base oil (PAO40) at four temperatures so as to achieve a wide range of fluid viscosities. The applied load was 3 N, corresponding to a mean pressure of 3.0 MPa. The viscosities of this fluid at the four test temperatures were 0.329, 0.128, 0.106 and 0.032 Pas at the test temperatures of 40, 60, 80 and 100°C respectively.

In Figure 1 it can be seen that friction coefficient remains high up to the largest bearing parameter value attainable. At very high bearing parameters there is a slight fall, possibly suggestive of the onset of mixed lubrication, or of thermal effects. It should be noted that the largest bearing index reached in the tests described in Part I, using ATF fluid with a fluid of viscosity 4.43 cP at 100°C, was *ca* 3×10^{-9} m.

There are two reasons why a steel/friction material contact fails to develop a full, separating hydrodynamic film even at high bearing parameter values. One is the porosity of the friction material. This allows fluid to leak out from the contact through the friction surface, thus inhibiting the build up of fluid pressure. Matsumoto *(3)* has shown that reducing the porosity of the friction materials has no effect on friction at slow sliding speeds but leads to more rapid friction drop at high speeds, indicating more facile transition to the mixed and hydrodynamic regimes.

The second reason, which has been stressed by Sanda *et al. (6)* and Eguchi and Yamamoto *(7)*, originates from the friction material morphology, which consists of loops of individual fibres, typically 30 to 50 μm diameter, protruding from a resin matrix. When loaded against a steel counterface, these protrusions result in a contact consisting of a low density of isolated "contact units", separated by wide valleys. Figure 2 shows an optical image of a typical dry, loaded contact while figure 3 shows an AFM topography map of one of the protruding fibres; both taken from Ingram *et al. (8)*. The steep sides of these contact units, combined with the fact that fluid can

escape from the valleys between the fibres due to porosity and side leakage, means that a fluid pressure cannot build up between the units to lift the surfaces apart. However because the contact units are themselves very small, it is difficult for a significant fluid pressure to develop within them since, according to hydrodynamic lubrication theory, the pressure within a bearing is proportional to the breadth of a plain bearing in the sliding direction (Stachowiak and Batchelor *(1)*).

From the above it is clear that the friction properties of a wet clutch contact will be determined by the lubricating film present in the contact units, so it is important to establish the operating conditions within these units.

The friction material used in this study consists primarily of 30 to 50 μm diameter, cellulose fibres, distributed within and held together by a phenolic resin matrix. The Young's modulus of the friction material is *ca* 0.10 GPa (Kimura and Otani *(9)*). This relatively low value is probably due in part to the porous nature of the material. The effective Young's modulus of the fibres is not known since there is a wide range of values for cellulose in the literature and also the fibres are coated with a phenolic resin of unknown thickness.

For the ball on flat contact used in the MTM sliding test described in Part I, the circular, apparent contact area is determined by the properties of the overall friction material. For the applied load of 3 N, and assuming a Poisson's ratio of 0.4 for the friction material, a Hertz radius of 0.56 mm is predicted, which is very similar to that observed experimentally. This corresponds to an apparent contact area of 1.0 mm2 and from this, the apparent mean contact pressure (the applied load divided by the apparent contact area) is *ca* 3.0 MPa.

Previous work by the authors has measured the fractional real area of contact and also the number of contact units per unit area as a function of applied pressure for the friction material used in the current study (Ingram *et al. (8)*). This shows that, at a mean applied pressure of 3 MPa, *ca* 4% of the apparent area is made up of contact units, with a density of *ca* 80 contact units/mm^2. This indicates that a representative contact unit has a load of 0.038 N, an area of 5 x 10^{-10} m^2 and a mean pressure of 75 MPa. If this contact unit has circular shape, it implies a contact radius of 12.5 μm and, if this is produced by elastic flattening of a 40 μm diameter sphere (a segment of protruding fibre), Hertz theory suggests that the reduced Young's modulus for fibre/steel combination is E^* = 0.28 GPa, where $E^* = \left(1-\nu_1^2\right)/E_1 + \left(1-\nu_2^2\right)/E_2$. E_1, E_2 and ν_1, ν_2 are the elastic moduli and the Poisson's ratio of the two surfaces, steel and resin-coated fibre.

.

A number of previous models of clutch friction have suggested that temperature rise plays a role in controlling friction (Marklund and Larsson *(10)*; Ohtani *et al. (11)*). In a recent study by the authors, the temperature of individual contact units for a sapphire surface sliding against friction material was measured using infrared emission microscopy (Ingram *et al. (12)*). This showed that the temperature rise of lubricated contact units remains below 5°C at sliding speeds up to 1 m/s, suggesting that flash temperature effects can be neglected below this speed in the current work.

These conditions of a representative contact unit are summarised in Table 1. Although derived for the MTM clutch simulator described and employed in Part I,

they are likely to be reasonably typical of wet clutch contact units in an LVFA or real component. As will be shown in the later in this paper, they can be used to estimate the prevalent fluid lubrication regime and fluid film thickness of wet clutch contact units.

Table 1. Representative contact conditions for a contact unit in the MTM sliding friction tests at u_s = 1 m/s	
Load, W	0.038 N
Reduced radius, $R' = R_{fibre}$	20 μm
Reduced elastic modulus, E^*	280 MPa
Entrainment speed, $U = u_s/2$	0.5 m/s
Pressure viscosity coefficient, α	10 GPa^{-1}
Dynamic viscosity, η	0.0025 Pas
Temperature (test temperature since flash temperature rise is less than 5°C)	100 °C

3. ORIGINS OF POSITIVE FRICTION SPEED CURVE

As indicated in the Introduction of this paper, the normally-expected friction *versus* speed behaviour of lubricated contacts is for friction to decrease initially with speed. This is because an increase in speed results in fluid entrainment into the contact and thus a transition from boundary lubrication through mixed to fluid film lubrication. Generally hydrodynamic and elastohydrodynamic fluid films have lower friction than boundary films, so the effect of this transition is to produce a fall in friction.

The desired, and generally achieved, frictional behaviour of wet clutches is the opposite of this, with friction increasing monotonically with sliding speed from low up to high speeds. Despite a great deal of research on wet clutch friction there is a surprising lack of clearly-expressed suggestions as to the origins of this behaviour. It is generally agreed that at, low sliding speed, a wet clutch operates in boundary lubrication and the friction is determined by the shear strength of the films produced by organic friction modifiers present in all ATFs. However why friction increases as sliding speed increases and why high speed friction can be enhanced by some detergent and dispersant additives, as described in Part 1, is still poorly understood. The various suggested origins for the observed behaviour of positive friction/speed response combined with high overall values of friction coefficient, can be grouped into three broad categories. These, and some more detailed possible mechanisms, are summarised in Table 2.

Table 2. Possible origins of the increase of friction with sliding speed in wet clutch contacts	
I.	A hydrodynamic film develops between the contact units at high speeds but this has a higher friction than the boundary film present at low speed
	A viscous film is present in the contact which gives high hydrodynamic friction [Kugimiya]

	A viscous film is present between asperities in the contact unit which contributes to friction at high speed [Sanda]
	Piezoviscous effects produce a non-Newtonian fluid whose shear strength increases with strain rate [Eguchi]
II. The contact units continue to operate in boundary lubrication to high speeds but there is an additional, superimposed, contribution to friction component which becomes significant at high speed	
	Shear of fluid film in the inter-contact regions makes a significant contribution at high sliding speeds [Devlin]
	Drag due to fluid passage into porous friction material makes a significant contribution at high sliding speeds [Devlin]
	Hysteresis losses in the friction material become significant at high sliding speeds
III. The contact units operate in boundary friction over the whole speed range, but the friction of this boundary film increases with sliding speed	

3.1 Hydrodynamic film friction contribution is greater than boundary film friction

Although boundary friction coefficients are normally much greater than hydrodynamic friction coefficients, this might not always be the case, especially if highly viscous films are present on rubbing surfaces. In the absence of such viscous films it is quite straightforward to estimate hydrodynamic friction values, based on the conditions present in a contact unit as listed in Table 1.

A number of researchers have provided maps for determining the prevailing fluid film lubrication regime that will be present in a contact, based on operating, geometry and materials properties. Assuming a circular contact based on a fibre segment of 40 μm diameter against a flat, these indicate that, if a fluid film does form, the contact will operate in the isoviscous elastic hydrodynamic regime over the whole sliding speed range from 1 mm/s to 2 m/s (Hamrock and Dowson *(13)*). Equations are available to predict both film thickness and friction coefficient (de Vicente *et al. (14)*) for this regime and figure 4 shows predicted film thickness and friction coefficient *versus* sliding speed for an individual, representative contact unit. Even assuming fully-flooded conditions, the predicted central hydrodynamic film thickness is less than 4 nm up to a sliding speed of 1 m/s, while the friction coefficient is less than 0.01. It should be noted that the root mean square roughness of the steel balls is *ca* 10 to 12 nm. From this it appears that the levels of friction coefficient measured in sliding friction material/steel contacts at high speeds are far too high to be explained in terms of the generation of a thin hydrodynamic film in the contact units.

However a much larger hydrodynamic friction value might result if a very thin, highly viscous liquid film were present on one or both of the rubbing surfaces. Kugimiya has suggested that additives that raise friction at intermediate and high speeds, such as detergents, may increase the viscosity of the fluid adjacent to the surfaces, so leading to a friction increase (Kugimiya *(19)*).

To test this possibility, some numerical solutions of a lubricated contact unit were made using the generalised Reynolds equation. This equation is similar to Reynolds equation but with viscosity expressed as integrals through the film thickness at each

location, so allowing viscosity to vary with distance from the solid surfaces. It was developed by Dowson *(20)* and applied later by Wen *et al. (21)* to analyse systems with layered viscosity. Appendix A describes the equations for pressure and shear stress used and provides some details of the solution method employed.

A single, lubricated contact unit was considered, with the truncated sphere on flat geometry described in section 2 of this paper, *i.e.* a 20 μm radius sphere having a circular 12 μm radius truncation, loaded against a smooth, steel flat. Rigid conditions were assumed and two different hypothetical viscosity profiles adjacent to both surfaces were considered as shown in Fig. 5. In these, the ordinate is the relative viscosity, *i.e.* the ratio of the viscosity at a given distance from the surfaces to the bulk fluid viscosity. The surface viscosity models considered are a thin layer of highly viscous fluid, (i) where viscosity decays stepwise from the surface and (ii) where it decays linearly.

Figures 6 and 7 show predicted film thickness and predicted friction coefficient *versus* sliding speed for the two assumed viscosity profiles. It can be seen that, as expected, the viscous films boost the fluid film thickness. Their impact on friction coefficient is interesting. They increase friction coefficient in the low speed region but as speed increases, the friction then falls back quite sharply to the isoviscous value as the contact ceases to be fully-filled with viscous fluid.

A related, viscous surface film mechanism was proposed by Sanda who considered the balance of boundary and hydrodynamic friction within a contact unit. He took into account the roughness of the steel counterface within the contact unit and concluded that the friction due to hydrodynamic shear increases more rapidly than its contribution to load support and thus film thickness in the unit (Sanda *et al. (6)*). This implied that the boundary friction at low speeds might be augmented by an additional, and increasing, hydrodynamic contribution as the speed was raised. The sliding speeds studied by Sanda were, however, much higher than those used in the current study.

Eguchi *et al. (7)* analysed wet clutch friction in terms of the Eyring shear thinning model for fluid flow, often employed in modelling piezoviscous elastohydrodynamic lubrication and suggested that, for a confined fluid film, increasing speed might produce an effective shift in the transition from fluid to quasi-solid behaviour, resulting in an effective viscosity increase in the contact and thus a friction increase. It is possible to estimate the likely contribution of pressure to effective viscosity and thus friction in the contact units based on the conditions listed in Table 1. Using the Barus equation, at a mean contact unit pressure of 75 MPa and a pressure viscosity coefficient of 10 GPa^{-1}, the mean viscosity in the contact, and thus the friction, should only increase by a factor of two. This would not be enough to explain the levels of friction measured, unless viscous surface films were also formed.

3.2 An additional friction component at high sliding speed

A number of authors have proposed that friction increases with sliding speed due to an additional, speed-dependent, drag contribution which becomes more significant as speed increases (Miyazaki *(5)*; Devlin *et al. (15)*). In this model, the principle component of friction is considered to be boundary friction at the contact units, but, as

the sliding speed is raised, this is augmented by, in the terminology of (Devlin *et al. (15-16)*), a "thin film" friction component. The precise nature of the latter is not clear but it has been proposed that it may originate from shear of fluid in the non load-bearing regions between the contact units or from flow of fluid into the porous friction material.

Both of these possibilities can be analysed. The maximum friction due to shear of fluid in the non-contact unit regions can be estimated from;

$$F = \tau A_{nc} = \eta \frac{u_s}{h_{nc}} A_{nc} \tag{1}$$

where h_{nc} is the mean separation between the steel ball surface and the friction material surface in the non-contact unit regions, while A_{nc} is the oil-filled area of these regions. Since the contact units result from protruding segments of 40 μm diameter fibres, as shown in Fig 3 a reasonable of h_{nc} is 10 μm, while, because the contact units occupy only a small fraction of the apparent area, A_{nc} can be taken to be the apparent ball on disc contact area (≈ 1 mm^2), assumed a fully flooded contact. Equation 1 then predicts the total friction from the non-contact unit regions to be *ca* 0.25 mN at 1 m/s. This is much lower than the measured friction of *ca* 0.45 N at the applied load of 3 N. Even if a separation of only 1 μm were assumed in the non-contact unit regions, the friction contribution from this source would still be less than 1% of the total. It should also be noted that the work of Sanda *et al. (6)* suggests that the sliding wet clutch contact is unlikely to be fully flooded. These estimates would, of course, change if the fluid filling the non-contact regions was significantly greater than that of the bulk fluid, perhaps due to additive concentration or deposition.

The contribution to friction from fluid entering the porous friction disc can be estimated from momentum exchange. Assuming the fluid enters the moving friction disc from an initially stationary state, then;

$$F = \dot{Q} \rho u_s \tag{2}$$

where $\dot{Q}$ is the flow rate into the friction material, ρ the fluid density and u_s the speed of the friction disc. The flow rate is difficult to estimate precisely, but assuming that it is controlled by the radial flow through the friction material layer, at radius r in the circular contact it will be;

$$\dot{Q} = \frac{2\pi r k_r t}{\eta} \frac{dp}{dr} \tag{3}$$

where k_r is the lateral permeability of the friction material, t the thickness of the friction material layer, dp/dr is the radial pressure gradient and η the fluid dynamic viscosity. The pressure in the non-contact unit regions in a continuously slipping clutch is not known but is likely to be very low since the applied load is supported at the contact units. Assuming, for simplicity, that pressure falls linearly from the maximum theoretical Hertz pressure, p_{max} at the centre of the contact to the zero at the perimeter so dp/dr = p_{max}/a where a is the Hertzian contact radius, then based on

values of p_{max} = 5 MPa, $r = a$ = 0.5 mm, t = 0.5 mm, η = 0.0025 Pas and k_r = 0.3 x 10^{12} m^2, the value of $\dot{Q}$ = 0.4 x 10^{-6} m^3/s. The value of k_r is taken from Darcy number values of lateral permeability of friction material determined by (Chavdar *(17)*). Based on this value of $\dot{Q}$, Eq. 2 predicts a contribution of this fluid entering the disc to friction of 0.3 mN. This value of $\dot{Q}$ is almost certainly a considerable overestimate but, even so, the calculated contribution to friction is less than 0.1% of the total.

An additional possible contribution to sliding friction at high speed might be viscoelastic dissipation in the friction material. This was briefly explored in the current study using the bidirectional sliding/rolling method described in [18], which can separate sliding and rolling ratio components. However this showed no significant rolling friction component for the friction material coated disc used.

The above discussion and analysis does not wholly preclude any of the suggested mechanisms. Indeed most are difficult to refute because they are based on the concept that friction-enhancing additives, such as detergents and dispersants, produce surface films of unknown viscosity and thickness. However in the next section the authors identify a relatively simple model, in accord with the literature, to explain the friction/speed behaviour of wet clutch without recourse the thick boundary film effects.

4. BOUNDARY FRICTION INCRESES WITH SLIDING SPEED

The third possible reason listed in Table 2 why friction coefficient might increase with sliding speed in a wet clutch contact is simply that the contact always operates in boundary lubrication but the boundary friction coefficient increases with sliding speed.

The authors were surprised to find no reference to this possibility in the wet clutch literature since it is well-established that self-assembled and Langmuir Blodgett surfactant monolayers can give such behaviour at slow sliding speeds, as can some polymers (Briscoe and Evans *(22)*; Chugg and Chaudhri *(23)*; Unal *(24)*; Jia *(25)*; Myshkin *(26)*). Figure 8, taken from Briscoe and Evans *(22)* shows a plot of the variation of the shear strength with log(sliding speed) for the sliding contact of stearic acid-coated mica surfaces. The shear strength was calculated by dividing the measured friction force by the measured area of contact of the very smooth surfaces used.

As shown in Fig. 8, and confirmed by other researchers, there is a linear/logarithmic friction-speed dependence of the form;

$$\tau = \tau_o'' + \theta \log_e u_s \qquad (4)$$

with the constants τ_o'' and θ being dependent on the pressure, temperature and the nature of the boundary film.

Clearly this implies a friction coefficient that also varies with log(sliding speed), *i.e.*

$$\mu = (\tau_o'' + \theta \log_e u_s)\frac{A_c}{W} \quad (5)$$

where A_c is the real contact area and W the applied load.

Figure 9 shows plots of friction coefficient versus log(sliding speed) for the long chain acid solution results reported in Part I, Fig. 7a. It can be seen that these give straight lines with gradient 0.0106. Since A_c/W = 1.3 x 10^{-8} Pa^{-1}, this implies a value of θ in Equ. 7 of 0.8 MPa. Briscoe and Evans measured a slope of 0.42 MPa for stearic acid on mica but at a different pressure and temperature.

In Fig. 10, the friction coefficients of other friction modifier solutions and also the formulated ATF are plotted in linear/log form. These also show linearity, with values of τ_o'' and θ that vary depending on the fluid used.

Briscoe and Evans showed that equation 4 can be derived from Eyring's model for thermally activated rate processes in fluid flow (Eyring *(27-28)*). This can be simply understood by considering the rate of molecular rearrangement of the adsorbed film as follows.

When two surfaces with adsorbed layer of densely packed FM-type molecules slide relative to one another under load, the sliding will occur between the methyl groups on the end of the alkyl chains of the FMs. There will be some interpenetration between the two FM layers, so when the molecules slide past one other, they will do so by minimizing the repulsive interactions between the approaching molecules. The molecules may minimize the repulsive forces by translational, rotational and conformational configuration changes (Kong *et al. (29)*). At higher speeds the molecules have less time to change their configurations, so the intermolecular repulsive forces between the sliding layers are increased. This leads to higher shear strength of the boundary films with increasing speed. In this model the gradient θ is inversely proportional to the stress activated volume, which is the size of segment that moves in the unit shear process.

Briscoe and Evan's thermally activated friction model also derives expressions for the dependence of shear stress on pressure and on temperature. The predicted dependence on temperature is;

$$\tau = \tau_o' + \beta T \quad (6)$$

where τ_o' and β are constants and T is the temperature. Figure 11 shows a plot of shear strength (calculated from measured friction coefficient assuming A_c/W = 1.3 x 10^{-8} Pa^{-1}) *versus* temperature at a sliding speed on 0.01 m/s for the two longer chain acid solutions. It can be seen that equation 6 is obeyed, with a value of β of -0.03 MPa/°C.

The reason that the apparent similarity in behaviour between wet clutch friction behaviour and that of work using Langmuir-Blodgett and self-assembled monolayers has not been previously highlighted may be that the latter studies were carried out at

very low sliding speeds, typically 1 μm/s to 1 mm/s, which were essential to prevent the formation of hydrodynamic films with the smooth surfaces used. However if a contact were to remain in the boundary lubrication regime to higher speed, the shear strength should continue to follow a linear/logarithmic speed dependence, at least until thermal effects become significant.

An increase of boundary friction with speed has been seen with long alkyl chain ZDDPs (though not short chain ones) at low speeds (Aoki *et al. (30)*) and also with a linear alkyl chain overbased calcium sulphonate dispersants (Topolovec *et al. (31)*). Both of these types of additive form a very rough surface films (of zinc phosphate and calcium carbonate respectively), thus extending the range of boundary lubrication regime to higher than normal speeds.

Based on the above, the authors consider that the most likely origin of the positive friction/sliding speed relationship seen with formulated ATFs and model blends containing organic friction modifiers is simply that they operate in primarily boundary lubrication throughout the whole sliding speed range and that the boundary friction coefficient increases slowly with sliding speed, as is characteristic of organic friction modifier films.

With this mechanism in mind, it is now possible to consider the impact of additives on the friction properties of ATF. The role of the organic friction modifier is clearly to provide a low shear strength film of the surface, strong enough to withstand very low speed or static conditions, while also having the desired positive shear stress/sliding speed behaviour characteristic of such additives. However, although the friction should increase with speed it is also important that the friction be as high as possible over the whole sliding speed range. This means that the friction modifier should not be too effective in reducing friction. This is seen in Figs. 9 and 10, where it can be seen that the more effective friction modifiers lower the friction curve over the whole speed range; *i.e.* they reduce the value of τ_o'' in Eq. 4.

It is illuminating in this context to consider the friction behaviour of the blends of different chain length acids reported in Part I. Some of these are reproduced in Fig. 12, in linear/log form. It can be seen that the effect of adding the short chain acid is to progressively increase the constant τ_o'' and to reduce θ, thus increasing the friction. This is believed to reflect the fact that the incorporation of short chain acids into the boundary monolayer produces a more interpenetrating, and thus higher shear strength interface.

Based on this, it is probable that dispersants and detergents perform a similar role, *i.e.* they adsorb within the primarily friction modifier film to produce an irregular and more easily interpenetrated boundary interface, as shown schematically in Fig. 13, resulting in larger τ_o''. It is noteworthy that this effect occurs with succinimide dispersants, that have highly branched polyisobutyl groups, and branched alkyl sulphonate detergents. The latter are known to increase boundary friction whereas their counterpart linear alkyl sulphonates reduce friction (Kugimiya *(19)*; Kitanaka *(32)*; Shirahama *(33)*).

In recent years, lateral force microscopy has been used quite extensively to investigate the friction/speed behaviour of various types of surface at slow sliding speeds (Kiely and Houston *(34)*; Gnecco *et al. (35)*; Brewer *et al. (36)*; Tambe and Bhushan *(37)*). This has shown that a continuous increase in friction with speed tends to occur between non-interacting, hydrocarbon surfaces. When polar functional groups are present, such as –OH and –COOH, friction-speed dependence is characterised by a very rapid initial increase with speed, followed by a plateau or fall in friction. It has been suggested that this results from hydrogen bonds between the surfaces being broken and not having time to reform as the sliding speed is raised (Brewer *et al. (36)*).

5. FRICTION BEHAVIOUR OF BASE OIL AT LOW SPEED

One of the most striking observations in Part I was the very different low speed friction behaviours of base oil and fully formulated ATF fluid. For base oil, and also solutions of oleic acid and mixtures of short and long chain fatty acids with a preponderance of short chain component, friction was high at low speeds and decreased as speed was increased. By contrast, fully formulated ATF fluids and most model blends containing organic friction modifiers showed friction that was low at slow speeds and increased with increasing speed. At high speeds, all fluids tended to a similar level of friction. A similar difference between base oil and fully formulated ATF friction has been reported by Ito *et al. (4)* and Miyazaki and Hoshino *(5)*.

Initially this base oil behaviour was interpreted in terms of classical boundary lubrication, in which the lack of adsorbing species in base oil results in solid-solid adhesion at low speeds and thus high friction, whereas for the ATF and other friction modifier solutions, additives were presumed to form a boundary film to prevent such adhesion. However, as shown in Fig. 14, tests carried out in dry conditions, with no lubricant present, show friction that increases with speed, similar to the ATF but very different from the base oil. This suggests that the observed high friction at low speeds is actively produced by the base oil rather than simply reflecting the poor boundary lubricating properties of this fluid. (The increase in friction seen with dry friction material is not surprising since it has been seen with a number of polymer systems and is presumed to originate from the same activated shear mechanism as described in section 4 above.

Two alternative possible mechanisms for this base oil friction behaviour were considered by the authors. One is that, in dry lubrication, a transfer film of phenolic resin rapidly builds up on the steel counterface and that this results in the observed low friction at low speeds. However hydrocarbon liquid prevents such a transfer film, so that, in the absence of effective boundary lubricating additives resin rubs against steel to give high friction at low speeds. As the sliding speed is increased it is then presumed that a very thin film of weakly absorbed base oil (of monolayer proportions) is able to reduce friction even for the resin on steel contact.

Another possibility, favoured by the authors, is that the high friction seen at very low speeds with base oil results from a capillary effect that is lost at high speeds and when effective friction-reducing additives are present. It is envisaged that the fluid only partially wets one or both of the surfaces, so that fluid bridges the two surfaces locally

around the contact units but does not flood the whole contact, as shown schematically in Fig.15.

Some simple experiments were carried out to see if the contact is, in fact, filled with fluid. In each test, a 10 mm diameter friction material-coated disc was cleaned in hexane for 20 minutes, air-dried and then covered in lubricant. It was then loaded against a coated glass disc and an optical image of the resulting contact was taken through the glass using white light. The imaging method used is based on total internal reflection at the glass surface and is further described in Ingram *et al. (8)*. Figure 16 compares the images from contacts using a dry disc and one initially covered in base oil. Locations where either friction material or liquid is in contact with the glass appear as darker regions due to total internal reflection, while areas where air is present remain light. For dry conditions, contact is confined to tiny contact units, typically 20-40 μm diameter and comprises a few percent of the total area, as noted in previous work (Eguchi and Yamamoto *(7)*; Ingram *et al. (8)*). For the lubricated case, however, fluid bridges about 20% of the total area and is apparently randomly dispersed. It is probably collected around contact units and at other regions where the separation between the surfaces is very small. Similar partial coverage was seen with ATF and additive solutions but the method was not sensitive enough to differentiate behaviour of different fluids. Also it cannot be assumed that fluids will behave the same when the glass surface is replaced by steel. It is, however, clear that, even when surplus fluid it present, this may not fully fill the cavities between the loaded surfaces in static conditions, so that capillary effects are possible.

The presence of localised fluid bridges between the surfaces might, in principle, contribute to an increase in measured friction coefficient in two different ways, *via* an increase in effective load due to capillary pressure and/or *via* an increase in friction due to the need to move the wetting lines present.

The potential importance of the contribution of capillary pressure to friction in low load contacts, in particular in the AFM, has been stressed and analysed by a number of researchers (Tian and Bhushan *(38)*; Ouyan *et al. (39)*; Butt *et al. (40)*; Xiao and Qian *(41)*; Jones *et al. (42)*). For such an effect to produce the apparent increase in friction coefficient seen with base oil, the applied load of 3 N would need to be augmented by a capillary load of *ca* 0.65 N.

The contribution of capillary bridges to the effective load can be calculated by considering the Laplace pressure. This is the pressure difference across the curves air-liquid interface and is approximated by Chappuis *(43)* for thin films by:

$$\Delta p = \frac{\gamma_{LV}}{h}(-\cos\theta_1 - \cos\theta_2) \qquad (7)$$

where γ_{LV} is the interfacial tension of the liquid-air interface, h is the film thickness at the capillary surface and θ_1, θ_2 are the contact angles of the liquid-solid interface at the surfaces. In a contact with capillary bridge area A_b, the load support by the capillary effect is given by:

$$W = \gamma_{LV} \frac{A_b}{h}(-\cos\theta_1 - \cos\theta_2) \quad (8)$$

From equation 8 it can be seen that the capillary load is very dependent on the filled gap thickness, h that is assumed. If we assume partially-wetted conditions with $\theta_1 = 0$ (one surface wetted), $\theta_2 = 90°$, (one surface very poorly wetted), $\gamma_{LV} = 30 \times 10^{-3}$ J/m^2, and $A_b = 4 \times 10^{-8}$, corresponding to 4% of the nominal contact area in the sliding MTM tests (*i.e.* the same as the real area of contact), a gap of $h = 2$ nm would be required to generate a capillary load of 0.65 N. It is not unreasonable to assume that the contact units will be surrounded by such regions of small gap, especially since protruding fibres will tend to have a small curvature with respect to the counterface along the fibre length. There will also be some regions where protruding fibres approach close to the counterface without forming direct contact but are able to be bridged by a thin film of fluid.

Another possible contribution of bridging liquid to friction is the force needed to move wetting lines (de Gennes *(44)*; Sedev *et al. (45)*; Blake *et al. (46-47)*). A wetting line, which is the boundary of the solid/lubricant/air junction, requires a force to move it. This force is related to the change in contact angle from its stable, static contact angle to a dynamic contact angle (Blake *(47)*):

$$F_w = \gamma_{LV}(\cos\theta_S - \cos\theta_D)L \quad (9)$$

where θ_S is the static contact angle, θ_D is the dynamic contact angle and L is the wetted line length. Sedev *et al. (45)* have shown that the dynamic contact angle is dependent on the speed of the wetting line.

Assuming $\theta_s = 90°$ and $\theta_D = 110°$, Equ. 9 indicates that the length of wetting line needed to produce an addition to the friction force of 0.1 N (about 20% of the high speed friction force) would be 10 m. Even with the very irregular pattern of the liquid bridges shown in Fig. 16, this seems unlikely to be present in a contact of nominal area 10^{-6} m. This suggests that moving wetting lines probably do not contribute significantly to friction.

Some ancillary friction tests were carried out to test the possible impact of wetting on low speed friction. The friction material MTM discs were pre-treated using oxygen plasma cleaning just prior to testing. This is known to have the effect of oxidising organic surfaces to render them temporarily hydrophilic (Pykonen *et al. (48)*) and thus change their wetting properties. Figure 17 shows a series of friction tests using such a treated disc, lubricated with the base oil. The friction at low speeds was initially reduced but this effect was slowly lost over time. This suggests that wetting of the friction material does play a role in the low speed friction behaviour.

Tests were also carried out at different applied loads. Figure 18 shows three test results using hexadecane, which shows a similar increase of friction at low speeds to that produced by the Group III base oil. It can be seen that the low speed friction coefficient increases as the applied load is reduced, which is consistent with there being an additional load at low speed due to capillary pressure.

Based on the above, it appears possible that the very low speed friction seen with base oil and also some other fluids such as oleic acid solution may arise from an increase in the effective load originating from fluid partially bridging the steel/friction material surfaces. As the speed is raised these bridges are disturbed so the effect is progressively lost. Addition of organic friction modifiers either alters the wetting behaviour to remove the additional loading, or simply reduces low speed friction due to an adsorbed film even though load remains enhanced, or some combination of the two.

6. CONCLUSIONS

This paper has considered the possible physical mechanisms underlying the characteristic friction/sliding speed behaviour of wet clutches, *i.e*. high friction that increases progressively with increasing sliding speed. Despite the importance of this friction behaviour in determining wet clutch performance, its origins are still not fully clarified in the literature, despite considerable previous research.

A crucial feature of wet clutch contacts is that the very rough, fibre-based morphology of the friction material results in the friction material/steel contact consisting of many, tiny contact units separated by regions where the gap between the friction material valleys and steel is relatively large. This large gap, coupled with the porosity of the friction material, means that it is impossible for a significant hydrodynamic pressure to be generated within the overall contact to separate the contact units. Furthermore, the very small size of the contact units means that negligible hydrodynamic film can build up within the contact units, at least up to a sliding speed of 1 m/s.

This means that the friction behaviour is controlled by the shear stress of the boundary lubricating films present on the steel and friction material surfaces within the contact units. These boundary lubricating films are created by the additives present in the ATF, the most important of which is the organic friction modifier, which provides the important characteristics of low friction at low speed and friction that increases with sliding speed. The authors suggest that this behaviour originates simply from the fact that the shear stress of most organic friction modifier boundary films increases with the logarithm of the sliding speed. This has been previously reported for Langmuir-Blodgett and self-assembled monolayers and has also been quite widely reported in molecular modelling work on monolayers and in the AFM literature. However it does not appear to have been previously considered in the context of ATFs and wet clutches.

The role of other “friction enhancing” additives used in ATFs, such as dispersants and detergents, is probably to partially disrupt the absorbed monolayer produced by the organic friction modifier so as to raise the latter’s friction over the whole speed range, while maintaining the required positive friction/log(sliding speed) gradient.

When friction material is rubbed against steel in dry conditions, friction is found to increase with increasing sliding speed. This means that the high friction measured at low speeds with base oil and some very weakly boundary-lubricating liquids is not simply due to lack of an effective boundary film. Instead it may be due either to the base oil inhibiting the formation of a resin transfer film from the friction material on

to the steel surface or, more likely in the authors' opinion, to capillary forces enhancing the effective load within the friction material/steel contact at low speeds.

8. ACKNOWLEDGEMENT

The authors gratefully acknowledge the support of Infineum Ltd. for the research described in this paper.

REFERENCES

(1) Stachowiak, G. W. and Batchelor, A. W. (2000), "Engineering Tribology," 2nd Edition, Butterworth-Heinemann, Boston, USA, ISBN 0 7506 7304 4.

(2) Sano, H. and Takesue, M. (1994), "Friction characteristics of wet clutch in the process of dynamic engagement," Jpn. J. Trib., **39**, 12, pp. 1567-1579.

(3) Matsumoto, T. (1993), "A study of the influence of porosity and resiliency of a paper-based friction material on the friction characteristics and heat resistance of the material," SAE Paper 932924.

(4) Ito, H., Fujimoto, K., Eguchi, M. and Yamamoto, T. (1993), "Friction characteristics of a paper-based facings for a wet clutch under a variety of sliding conditions," Trib. Trans., **36**, 1, pp. 134-138.

(5) Miyazaki, M. and Hoshino, M. (1988), "Evaluation of vibration-preventive properties of lubricating oils in wet friction plates and retention of such properties using a friction tester," SAE Paper 881674.

(6) Sanda, S., Nagasawa, Y., Suzuki, A., Hayashi, K. and Itoh, H. (1995), "Mechanism of friction of wet clutch with paper based facings. Part 1 Observation and modelling of facing surface during engagement," Proc. Int. Trib. Conf., Yokohama, Japan, pp. 1519-1524.

(7) Eguchi, S. and Yamamoto, T. (2005), "Shear characteristics of a boundary film for a paper-based wet friction material: friction and real contact area measurement," Trib. Int. **38**, pp. 327-335.

(8) Ingram, M., Spikes, H., Noles, J. and Watts, R. (2010), "The contact properties of a wet clutch friction material," Trib. Int. **43**, pp. 815-821

(9) Kimura, Y and Otani C., (2005) "Contact and wear of paper-based friction materials for oil-immersed clutches - wear model for composite materials." Trib. Inter. 38. pp. 943-950.

(10) Marklund, P. and Larsson, R. (2007), "Wet clutch under limited slip conditions – simplified testing and simulation," Proc. IMechE Part J: J. Eng. Trib. **221**, pp. 545-551.

(11) Ohtani, H., Hartley, R. J. and Stinnett, D. W. (1994), "Prediction of anti-shudder properties of automatic transmission fluids using a modified SAE No. 2 machine," SAE Paper 940821.

(12) Ingram, M. Reddyhoff, T. and Spikes, H.A. "Thermal behaviour of a slipping wet clutch contact." Submitted for publication in Trib Lett, March 2010.

(13) Hamrock, B. J. and Dowson, D. (1981), "Ball bearing lubrication," Wiley, New York, ISBN 0 4710 3553 X.

(14) de Vicente, J., Stokes, J. R., Spikes, H. A. (2005), "The frictional properties of Newtonian fluids in rolling-sliding soft-EHL contact," Trib. Lett. **20**, 3-4, pp. 273-286.

(15) Devlin, M. T., Tersigni, S. H., Senn, J., Turner, T. L., Jao, T. and Yatsunami, K. (2005), "Modelling friction contributions in step-automatic clutches," Proc. Int. Symp. Tribol. Vehicle Transmission, Tsukuba, Japan, pp. 125-135.

(16) Devlin, M. T., Tersigni, S. H., Senn, J., Turner, T. L., Jao, T. and Yatsunami, K. (2005), "Effect of friction material on the relative contribution of thin-film friction to overall friction in clutches," SAE Paper 2004-01-3025

(17) Chavdar, B. (2002), "A permeameter measuring normal and lateral permeability and an investigation on wet friction materials," Proc. 47th Int. SAMPE Symp., May 12-16, pp. 253-266.

(18) Vicente J. de, Stokes, J.R. and Spikes, H.A., (2006), "Rolling and sliding friction in compliant, lubricated contact." Proc. I.Mech.E. Ser. J **220**, pp. 55-63.

(19) Kugimiya, T. (2000), "Effects of additives for ATF on μ-v characteristics," Proc. Int. Trib. Conf., Nagasaka, Japan, pp. 1355-1360

(20) Dowson, D. (1962), "A generalized Reynolds equation for fluid-film lubrication" International Journal of Mechanical Science **4**, pp. 159-170

(21) Qingwen, Q., Yahong, H. and Jun, Z. (1998), "An adsorbent layer model for thin film lubrication," Wear **221**, pp. 9-14

(22) Briscoe, B. J. and Evans, D. C. B. (1982), "The shear properties of Langmuir-Blodgett layers," Proc. R. Soc. Lond. **A 380**, pp. 389-407

(23) Chugg, K. J. and Chaudhri, M.M. (1993), "Boundary lubrication and shear properties of thin solid films of dioctadecyl dimethyl ammonium chloride (TA100)," J. Phys. D: Appl. Phys. **26**, pp. 1993-2000.

(24) Unal, H., Mimaroglu, A., Kadioglu, U. and Ekiz, H. (2004), "Sliding friction and wear behaviour of polytetrafluoroethylene and its composites under dry conditions," Material and Design **25**, pp. 239-245

(25) Jia, B., Li, T., Liu, X. and Cong, P. (2007), "Tribological behaviours of several polymer-polymer sliding combinations under dry friction and oil-lubricated conditions," Wear **262**, pp. 1353-1359

(26) Myshkin, N. K., Petrokovets, M. I. and Kovalev, A. V. (2005), "Tribology of polymers: adhesion, friction, wear, and mass-transfer," Trib. Int. **38**, pp. 910-921.

(27) Eyring, H. (1935), "The activated complex in chemical reactions," J. Chem. Phys. **3**, pp. 107-115.

(28) Eyring, H. (1936), "Viscosity, plasticity, and diffusion as examples of absolute reaction rate," J. Chem. Phys. **4**, pp. 283-291.

(29) Kong, Y. C., Tildesley, D. J. and Alejandre, J. (1997), "The molecular dynamics simulation of boundary-layer lubrication," Molecular Phys. **92**, 1, pp. 7-18.

(30) Aoki, S., Suzuki, A. and Masuko, M. (2006), "Comparison of sliding speed dependency of friction between steel surfaces lubricated with several ZnDTPs with different hydrocarbon moieties," Proc. IMechE Vol. **220** Part J: J. Engineering Tribology, pp. 343-351.

(31) Topolovec-Miklovic, K., Reg Forbus, T. and Spikes, H. (2008), "Film forming and friction properties of overbased calcium sulphonates," Tribol. Lett. **29**, pp. 33-44.

(32) Kitanaka, M. (1992), "Friction characteristics of some additives in ATFs," Proc. 8th Int. Colloquium Tribology 2000, Germany, 22.8-1.

(33) Shirahama, S. (1994), "Adsorption of additives on wet friction pairs and their frictional characteristics," Jpn. J. Trib. **39**, 12, pp. 1479-1486.

(34) Kiely, J. D. and Houston, J. E. (1999), "Contact hysteresis and friction of alkanethiol self-assembled monolayers on gold," Langmuir **15**, pp. 4513-4519.

(35) Gnecco, E., Bennewitz, R., Gyalog, T., Loppacher, Ch., Bammerlin, M., Meyer, E. and Guntherodt, H. –J. (2000), "Velocity dependence of atomic friction," Physical Review Letters **84**, 6, pp. 1172-1175.

(36) Brewer, N. J., Beake, B. D. and Leggett, G. J. (2001), "Friction force microscopy of self-assembled monolayers: Influence of adsorbate alkyl chain length, terminal group chemistry, and scan velocity," Langmuir **17**, pp. 1970-1974.

(37) Tambe, N. S. and Bhushan, B. (2005), "Friction model for the velocity dependence of nanoscale friction," Nanotechnology **16**, pp. 2309-2324.

(38) Tian, X. and Bhushan, B. (1996), "The micro-meniscus effect of a thin liquid film on the static friction of rough surface contact," J. Phys. D: Appl. Phys. **29**, pp. 163-178.

(39) Ouyan, Q., Ishida, K. and Okada, K. (2001), "Investigation of micro-adhesion by atomic force microscopy," Applied Surf. Sci. **169-170**, pp. 644-648.

(40) Butt, H.J., Capella, B. and Kappl, M. (2005), "Force measurements with the atomic force microscope: Technique, interpretation and applications," Surf. Sci. Reports **59**, pp. 1-152.

(41) Xiao, X. and Qian, L. (2000), "Investigation of humidity-dependent capillary force," Langmuir **16**, pp. 8153-8158.

(42) Jones, R., Pollock, H. M., Cleaver, J. A. S. and Hodges, C. S. (2002), "Adhesion forces between glass and silicon surfaces in air studied by AFM: Effects of relative humidity, particle size, roughness, and surface treatment," Langmuir **18**, pp. 8045-8055.

(43) Chappuis, J. (1982), "Lubrication by a new principle: the use of non-wetting liquids," Wear **77**, pp. 303-313.

(44) de Gennes, P. G. (1985), "Wetting: statics and dynamics," Review of Modern Physics **57**, 3, pp. 827-863.

(45) Sedev, R. V., Budziak, C. J., Petrov, J. G. and Neumann, A. W. (1993), "Dynamic contact angles at low velocities," J. Colloid Interface Sci. **159**, pp. 392-399.

(46) Blake, T. D. and Shikhmurzaev, Y. D. (2002), "Dynamic wetting by liquids of different viscosity," J. Colloid Interface Sci. **253**, pp. 196-202.

(47) Blake, T. D. (2006), "The physics of moving wetting lines," J. Colloid Interface Sci. **299**, pp. 1-13.

(48) Pykonen, M., Sundqvist, H., Järnström, J., Kaukoniemi, O. –V., Tuominen, M., Lahti, J., Peltonen, J., Fardim, P. and Toivakka, M. (2008), "Effects of atmospheric plasma activation on surface properties of pigment-coated and surface-sized papers." Appl. Surf. Sci. **255**, pp. 3217-3229.

APPENDIX A Generalized Reynolds Equation

The Generalized Reynolds equation can be derived as follows, starting from the equilibrium of a fluid element. *x* is the sliding direction, *y* the transverse direction and *z* the direction through the film.

$\frac{\partial \tau}{\partial z} = \frac{\partial p}{\partial x}$ (analysis shown in x-direction; y-direction)

Integrate twice to find the velocity profile

$$\frac{\partial\left(\eta \frac{\partial u}{\partial z}\right)}{\partial z} = \frac{\partial p}{\partial x}$$

$$\frac{\partial u}{\partial z} = \frac{\partial p}{\partial x}\frac{z}{\eta} + \frac{1}{\eta}c_1$$

At this integration stage allow η to vary with z, so retain integral expressions.

$$u(z) = \frac{\partial p}{\partial x}\int_0^z \frac{z}{\eta}dz + c_1\int_0^z \frac{1}{\eta}dz + c_2$$

$u = u_1$ at $z = 0$

$u = u_2$ at $z = h$

$$u_2 = \frac{\partial p}{\partial x}\int_0^h \frac{z}{\eta}dz + c_1\int_0^h \frac{1}{\eta}dz c_1 + u_1$$

Using integral definitions;

$$J_1 = \int_0^h \frac{z}{\eta}dz, \quad J_0 = \int_0^h \frac{1}{\eta}dz, \; J_{1z} = \int_0^z \frac{z}{\eta}dz, \; J_{0z} = \int_0^z \frac{1}{\eta}dz$$

$$c_1 = \frac{-\frac{\partial p}{\partial x}J_1 + u_2 - u_1}{J_o}$$

$$u(z) = \frac{\partial p}{\partial x}J_{1z} + \left(\frac{-\frac{\partial p}{\partial x}J_1 + u_2 - u_1}{J_0}\right)J_{0z} + u_1$$

$$u(z) = \frac{\partial p}{\partial x}\left(J_{1z} - \frac{J_1}{J_0} J_{0z} \right) + u_1 \left(1 - \frac{J_{0z}}{J_0} \right) + u_2 \frac{J_{0z}}{J_0}$$

Assume $u_2 = 0$

$$u(z) = \frac{\partial p}{\partial x}\left(J_{1z} - \frac{J_1}{J_0} J_{0z} \right) + u_1 \left(1 - \frac{J_{0z}}{J_0} \right) \tag{A1}$$

Integrate velocity equation A1 to find the flow through a column of film

$$q_x = \int_0^h u(z) dz = \frac{\partial p}{\partial x}\left(\int_o^h J_{1z} dz - \frac{J_1}{J_0} \int_o^h J_{0z} dz \right) + u_1 \left(1 - \frac{1}{J_0} \int_o^h J_{0z} dz \right)$$

Using integral definitions

$$J_{ozh} = \int_o^h J_{0z} dz \,, \quad J_{1zh} = \int_o^h J_{1z} dz$$

$$q_x = \frac{\partial p}{\partial x}\left(J_{1zh} - \frac{J_1}{J_0} J_{ozh} \right) + u_1 \left(1 - \frac{1}{J_0} J_{ozh} \right)$$

$$\frac{\partial q_x}{\partial x} = \frac{\partial}{\partial x}\left(\frac{\partial p}{\partial x}\left(\frac{J_{1zh} J_o - J_1 J_{ozh}}{J_o} \right) \right) - u_1 \frac{\partial}{\partial x}\left(\frac{J_{ozh}}{J_0} \right)$$

Using definitions;

$$J = \frac{J_{1zh} J_o - J_1 J_{ozh}}{J_o} \qquad J_R = \frac{J_{ozh}}{J_1}$$

$$\frac{\partial q_x}{\partial x} = \frac{\partial}{\partial x}\left(J \frac{\partial p}{\partial x} \right) - u_1 \frac{\partial J_R}{\partial x}$$

Continuity of flow through a column of fluid

$$\frac{\partial q_x}{\partial x} + \frac{\partial q_y}{\partial y} = \frac{\partial}{\partial x}\left(J \frac{\partial p}{\partial x} \right) + \frac{\partial}{\partial y}\left(J \frac{\partial p}{\partial y} \right) - u_1 \frac{\partial}{\partial x}\left(J_R \right) = 0$$

Generalized Reynolds equation;

$$\frac{\partial}{\partial x}\left(J \frac{\partial p}{\partial x} \right) + \frac{\partial}{\partial y}\left(J \frac{\partial p}{\partial y} \right) = u_1 \frac{\partial}{\partial x}\left(J_R \right) \tag{A2}$$

To calculate shear stress

$$\tau_x = \eta \frac{\partial u}{\partial z} = \eta \left(\frac{\partial p}{\partial x} \left(\frac{\partial J_{1z}}{\partial z} - \frac{J_1}{J_0} \frac{\partial J_{0z}}{\partial z} \right) - \frac{u_1}{J_o} \frac{\partial J_{0z}}{\partial z} \right)$$

$$\frac{\partial J_{1z}}{\partial z} = \frac{z}{\eta}, \quad \frac{\partial J_{0z}}{\partial z} = \frac{1}{\eta}$$

$$\tau_x = \eta \left(\frac{\partial p}{\partial x} \left(\frac{z}{\eta} - \frac{J_1}{J_0} \frac{1}{\eta} \right) - \frac{u_1}{J_o} \frac{1}{\eta} \right)$$

At $z = 0$,

Surface shear stress equation;

$$\tau_{x(z=0)} = \frac{\partial p}{\partial x} \left(- \frac{J_1}{J_0} \right) - \frac{u_1}{J_o} \qquad \text{(A3)}$$

The 2D generalized Reynolds equation (equation A2 above) was solved using a computing equation based on central differences and a rectangular grid across the contact region. The central film thickness was adjusted iteratively until the load support of the film balanced the applied load. At the start of each iteration, the integral expressions J_0, J_1, J_{0zh}, J_{1zh} and thus J and J_R were recalculated. Finally, the friction force was calculated using equation A3 above.

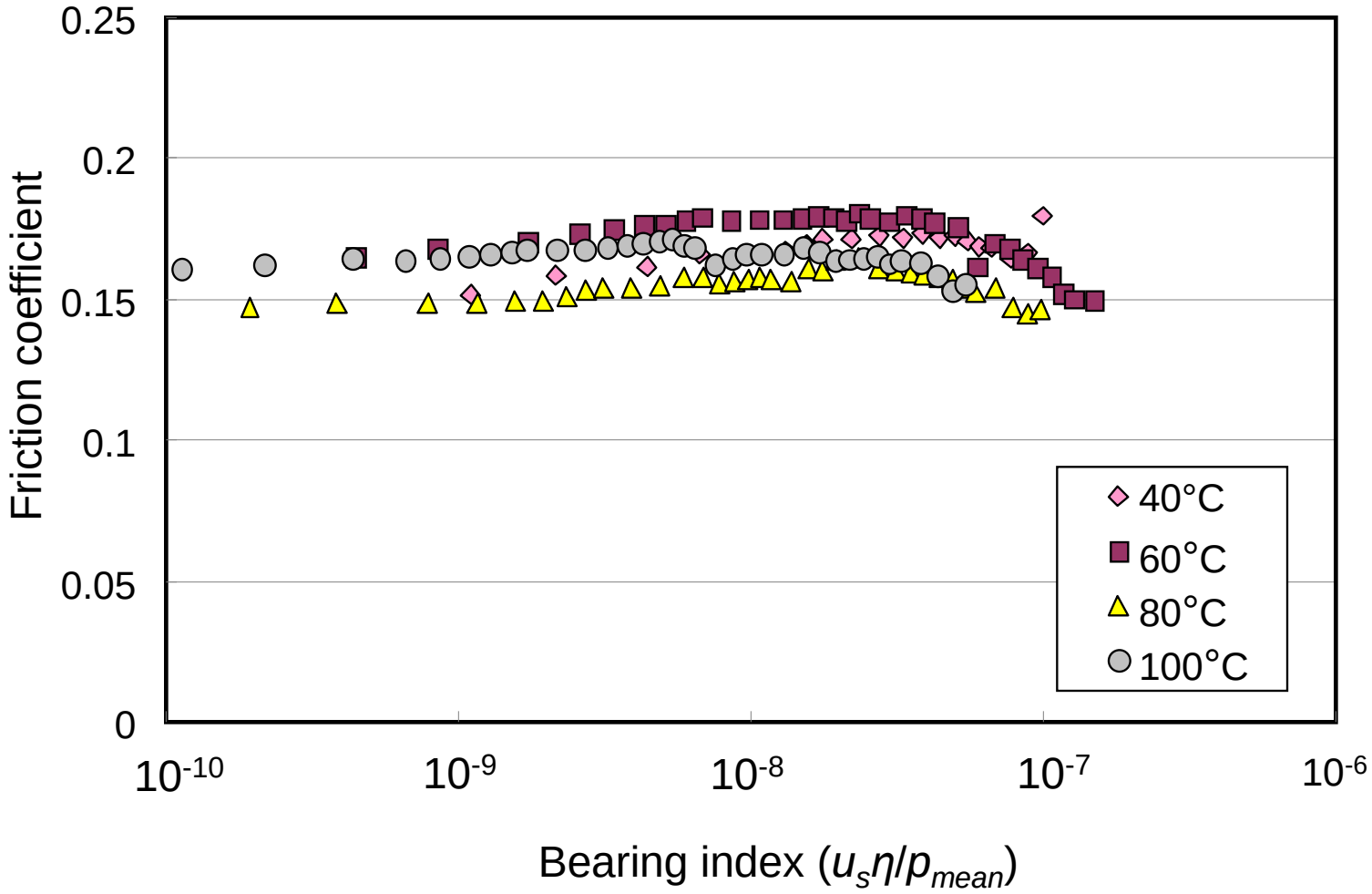

Figure 1. Friction coefficient *versus* bearing index for high viscosity base fluid tested at 3 N load and four temperatures

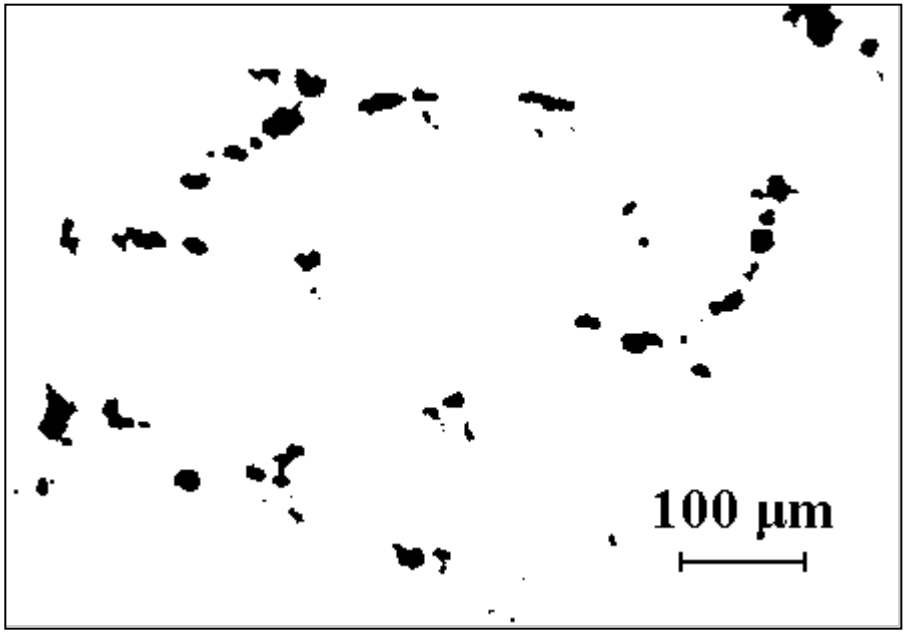

Figure 2. Optical image of part the contact area. Contact units shown as black; (reproduced from Ingram *et al. (8))*

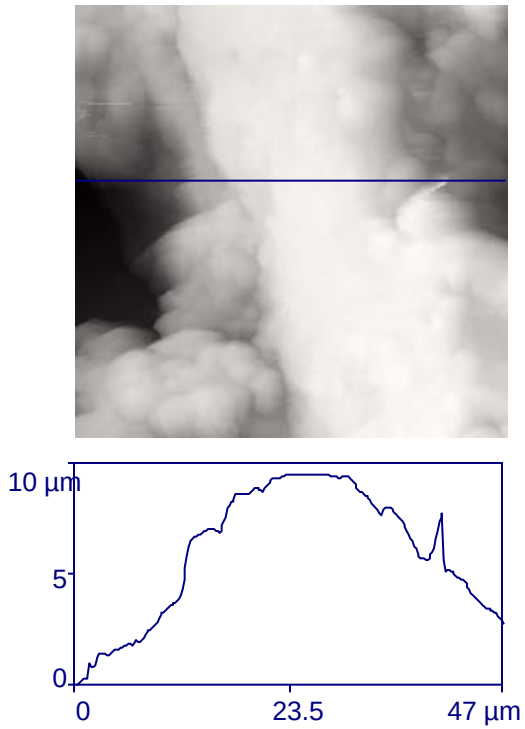

Figure 3. AFM image and profile of protruding fibre from fresh friction material surface; (reproduced from Ingram *et al. (8)*

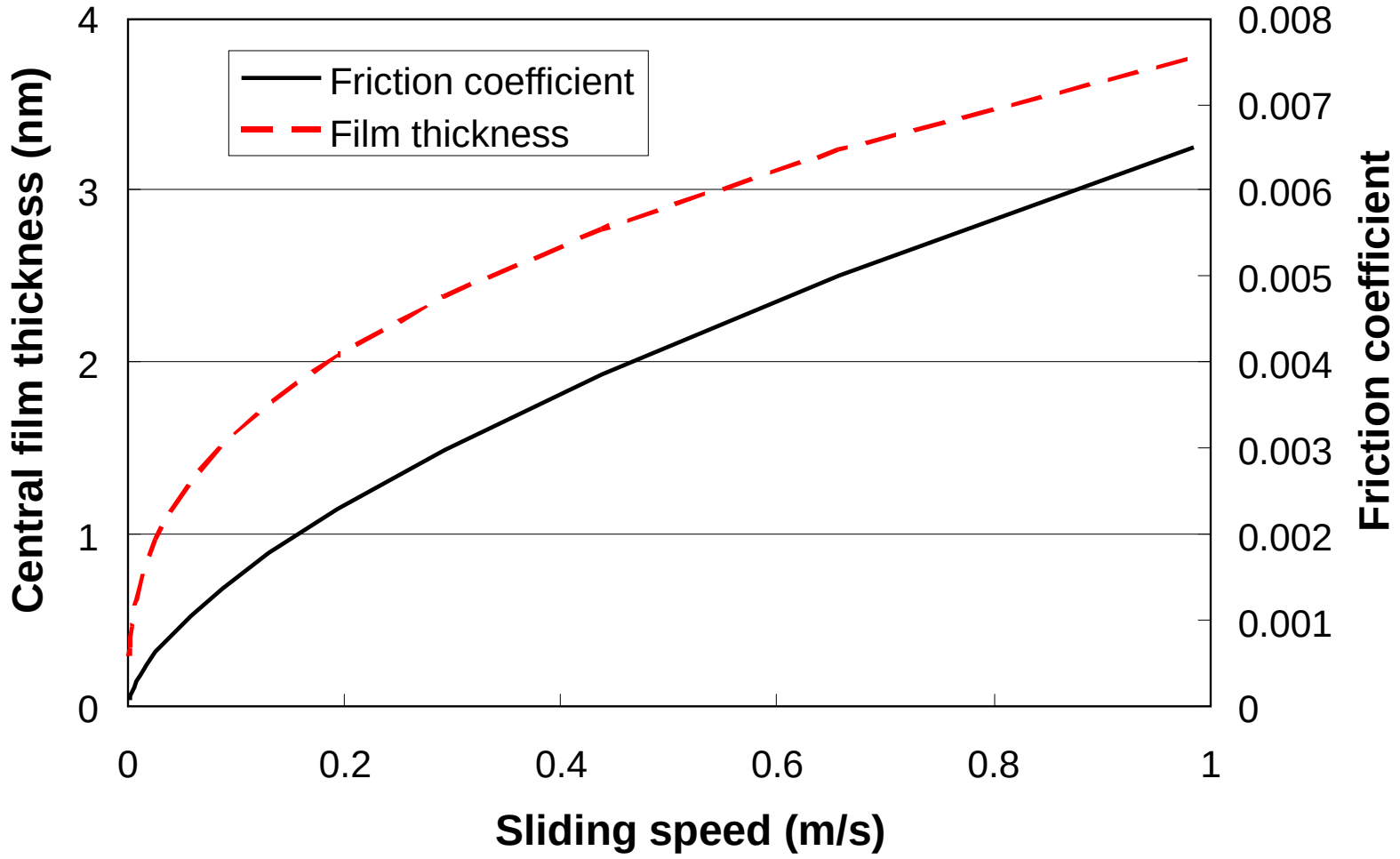

Figure 4. Theoretical central film thickness and friction coefficient for a soft EHL lubricated contact unit with properties described in Table 1.

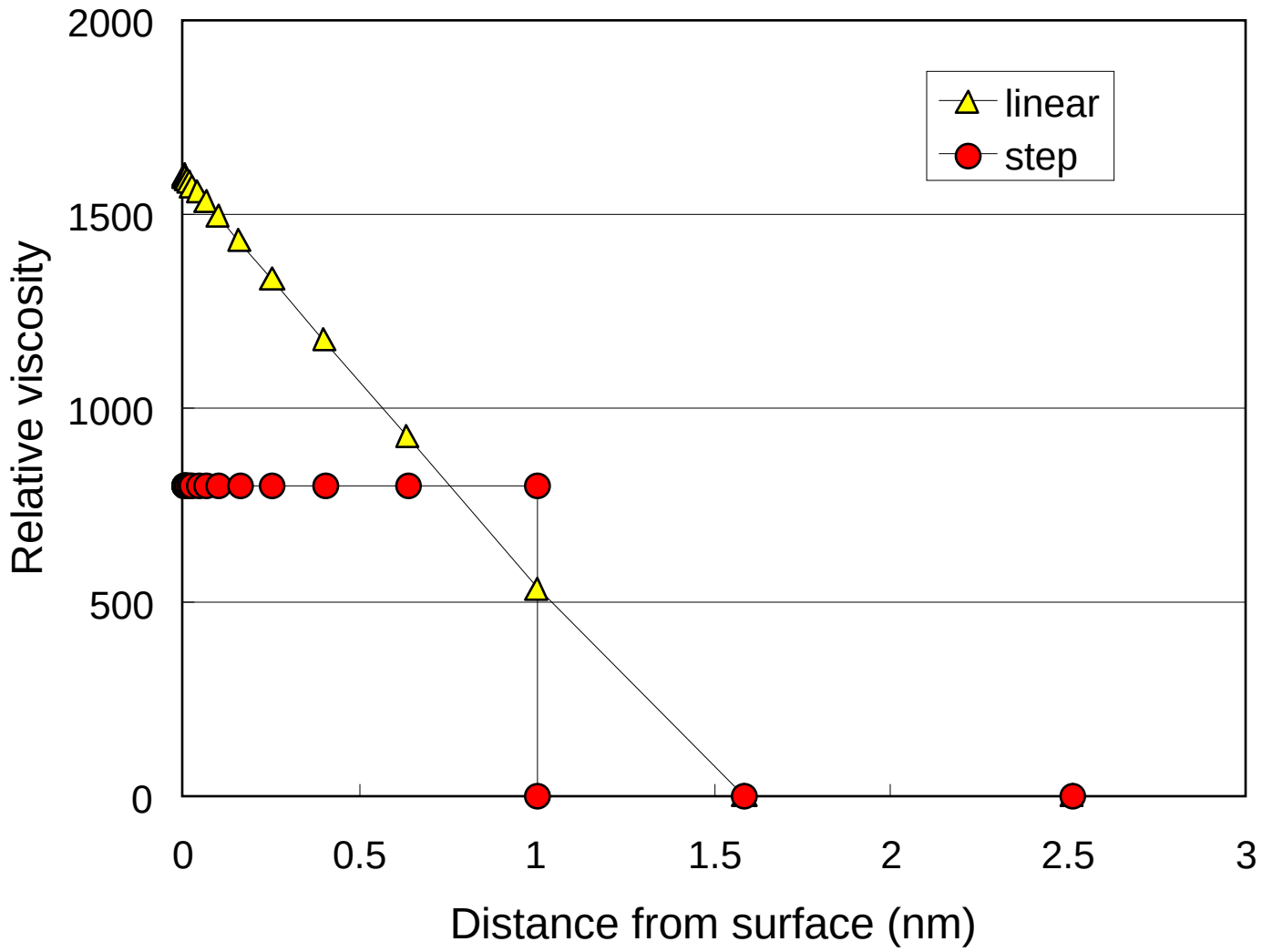

Figure 5. Viscosity profiles used in variable viscosity modelling

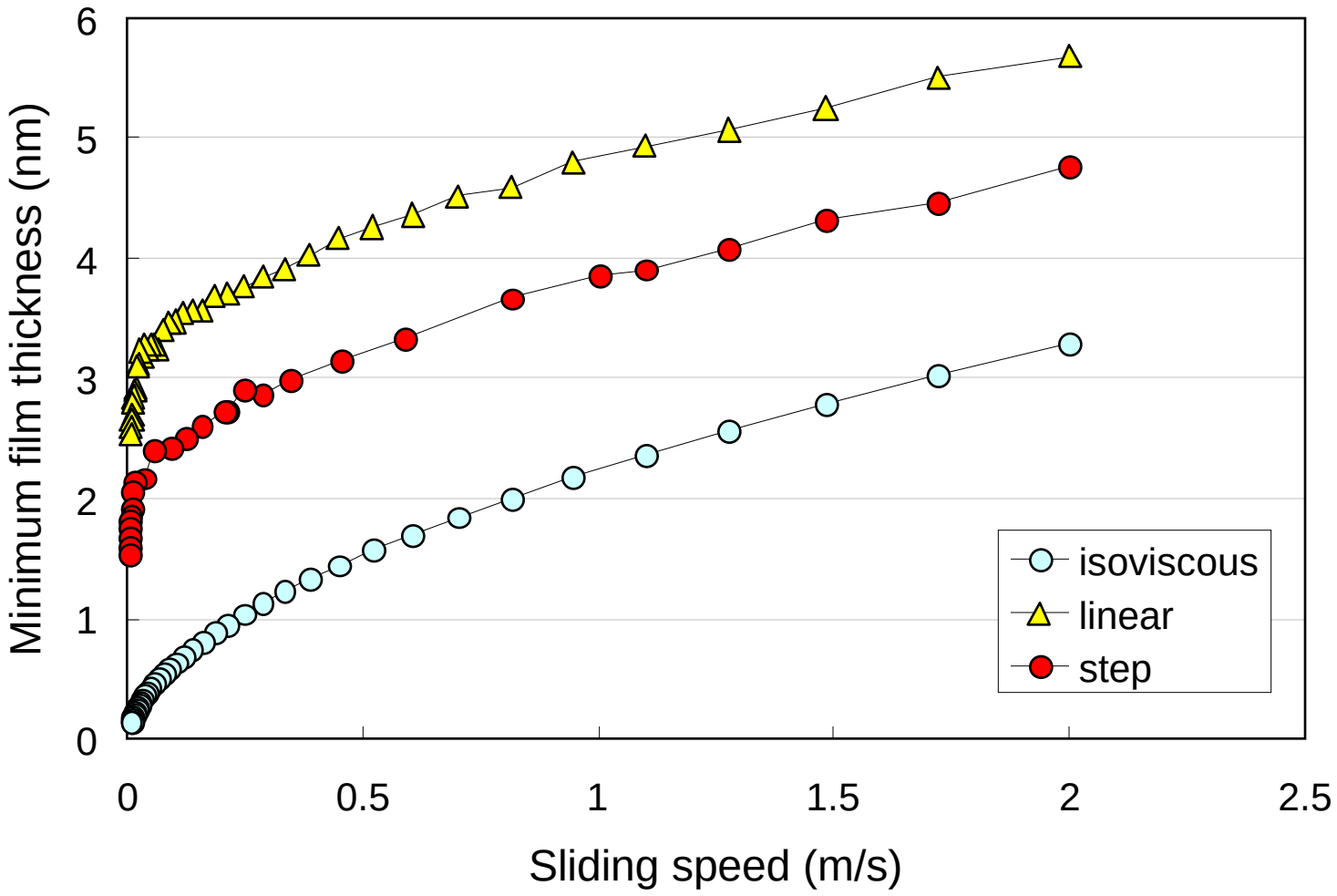

Figure 6. Theoretical minimum hydrodynamic film thickness based on different assumed viscosity profiles at the surfaces

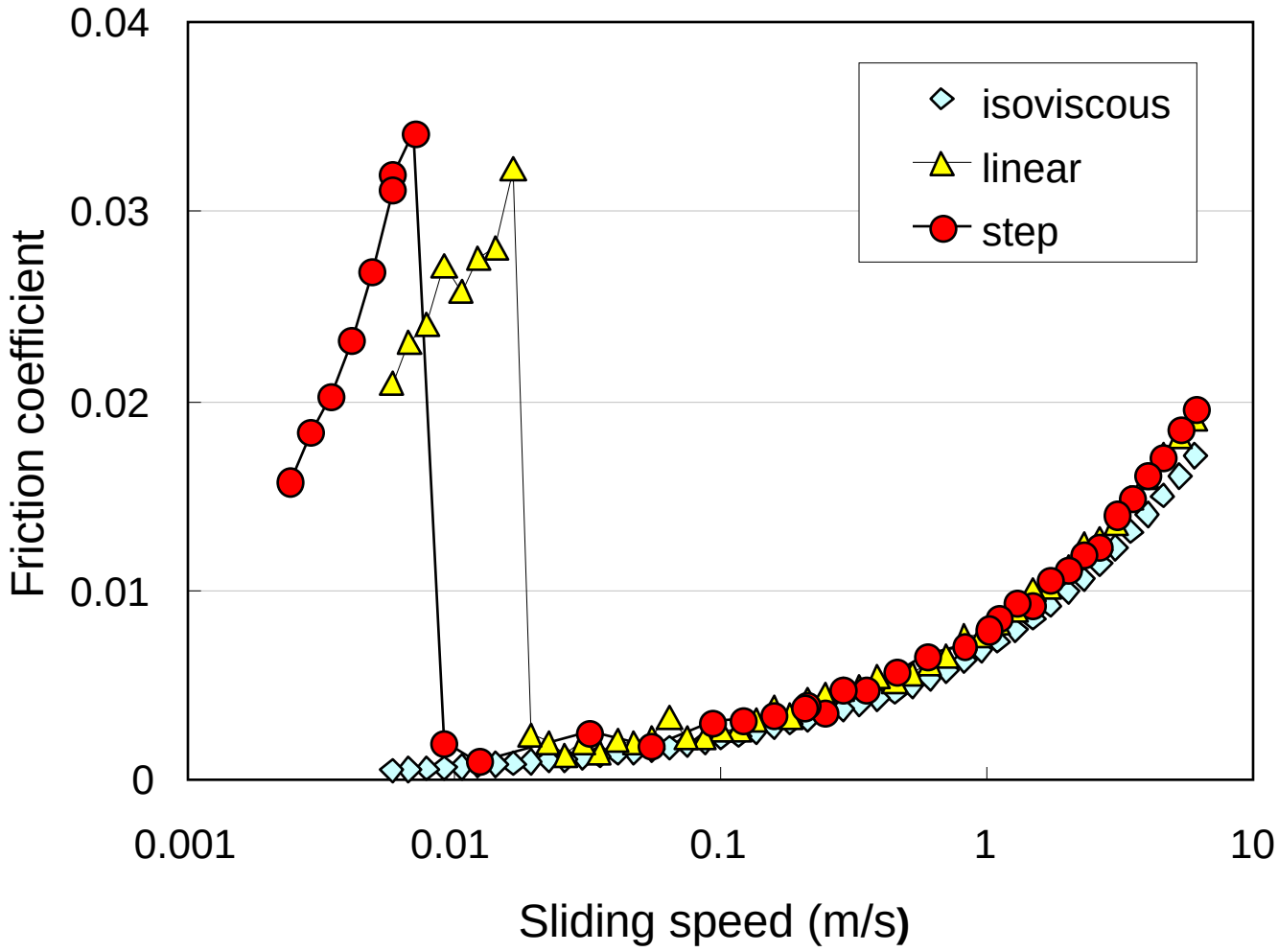

Figure 7. Theoretical hydrodynamic friction coefficients based on different assumed viscosity profiles at the surfaces

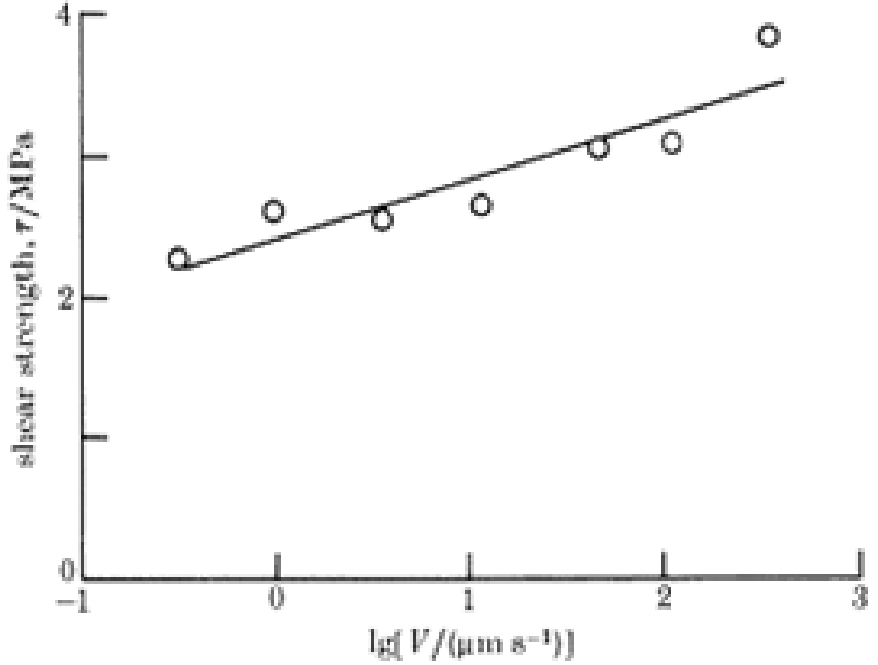

Figure 8. The variation of shear strength τ with sliding velocity V for stearic acid monolayers deposited from 10^{-4} M calcium chloride at pH 4.5, p_{mean} = 70 MPa, T = 21 °C; (reproduced from Briscoe and Evans *(22)*)

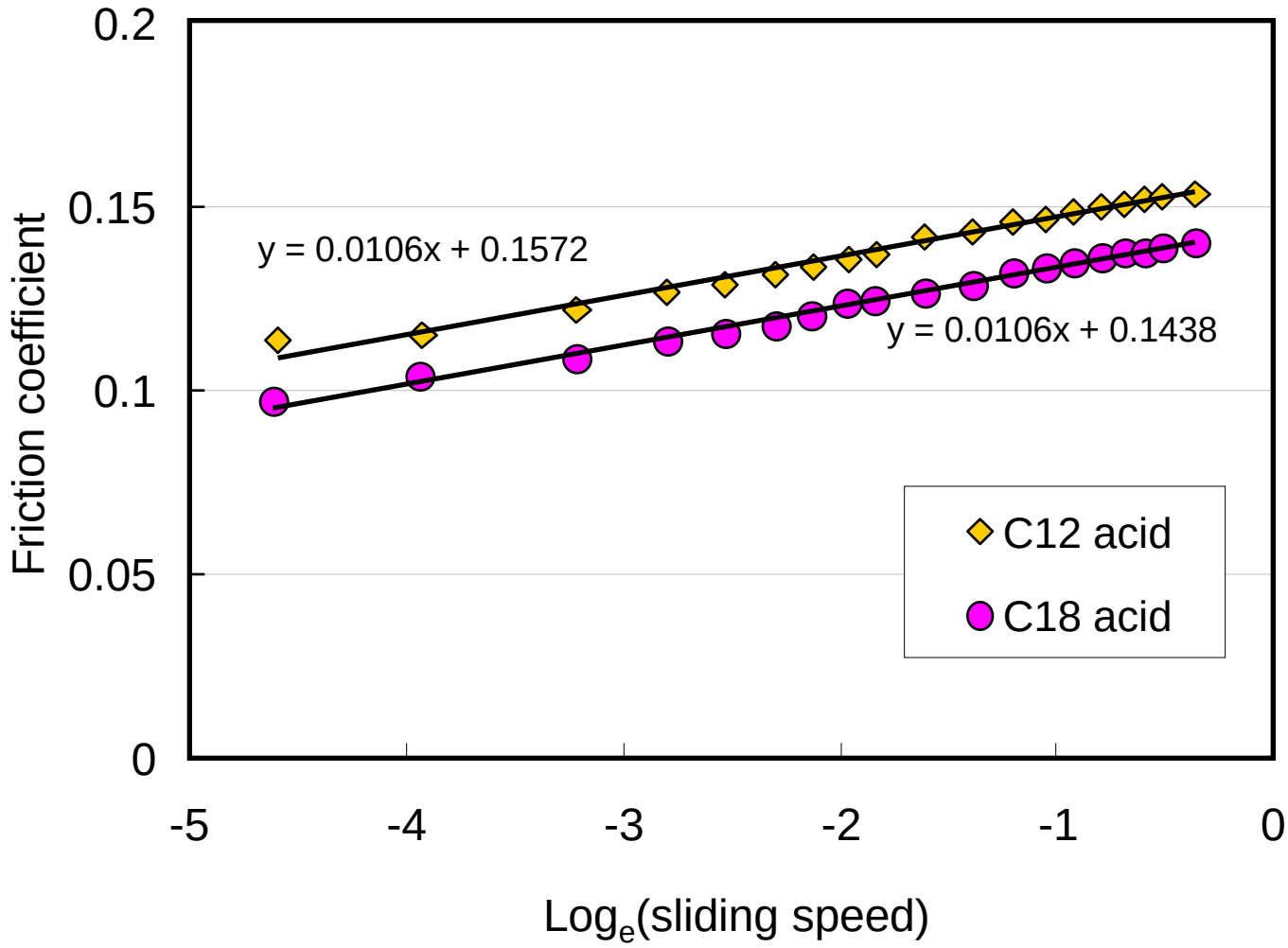

Figure 9. Linear friction coefficient *versus* logarithmic sliding speed plots for two carboxylic acid solutions at 100°C and 3 N load

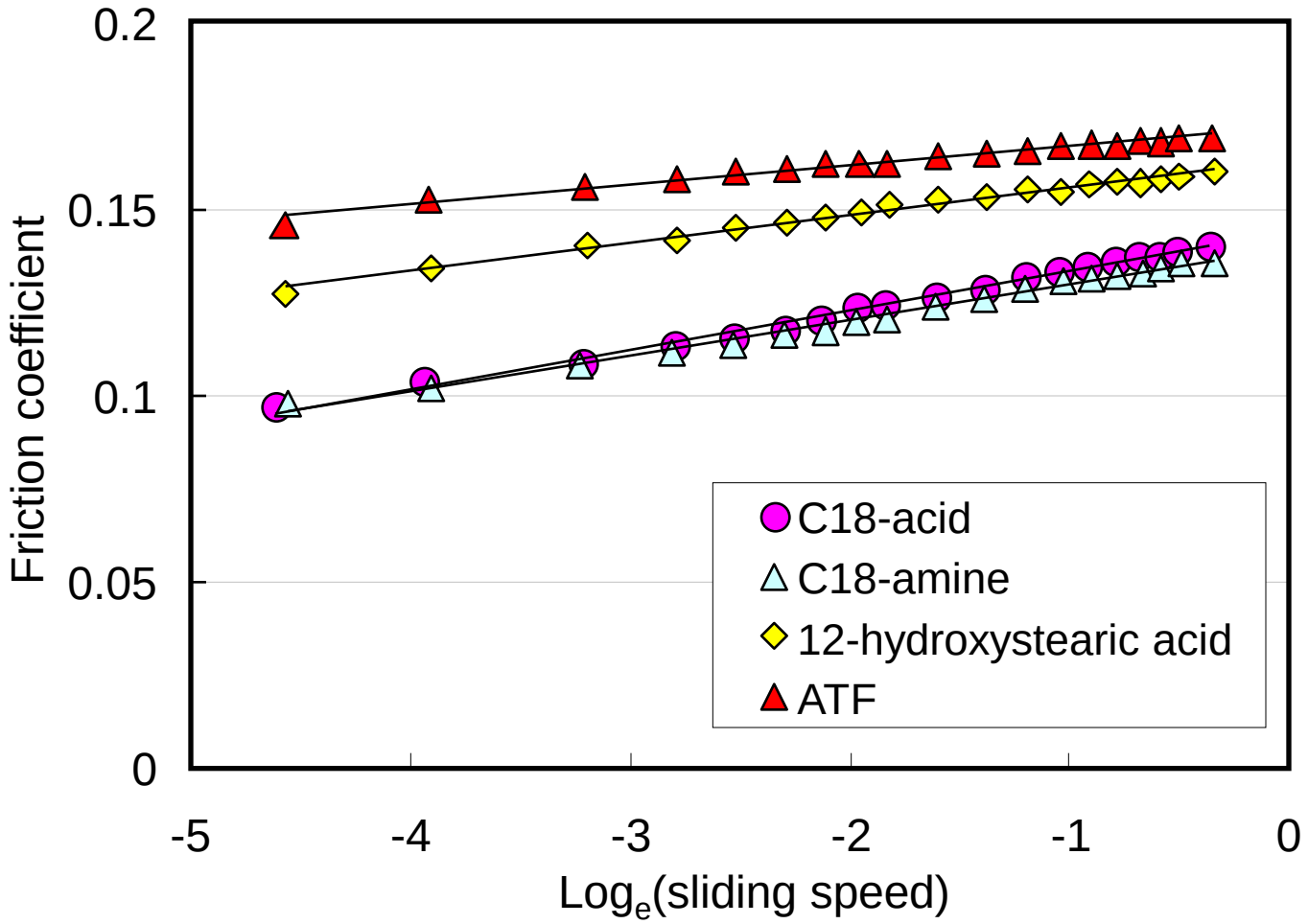

Figure 10. Linear friction coefficient *versus* logarithmic sliding speed plots for three friction modifier solutions and an ATF at 100°C and 3 N load

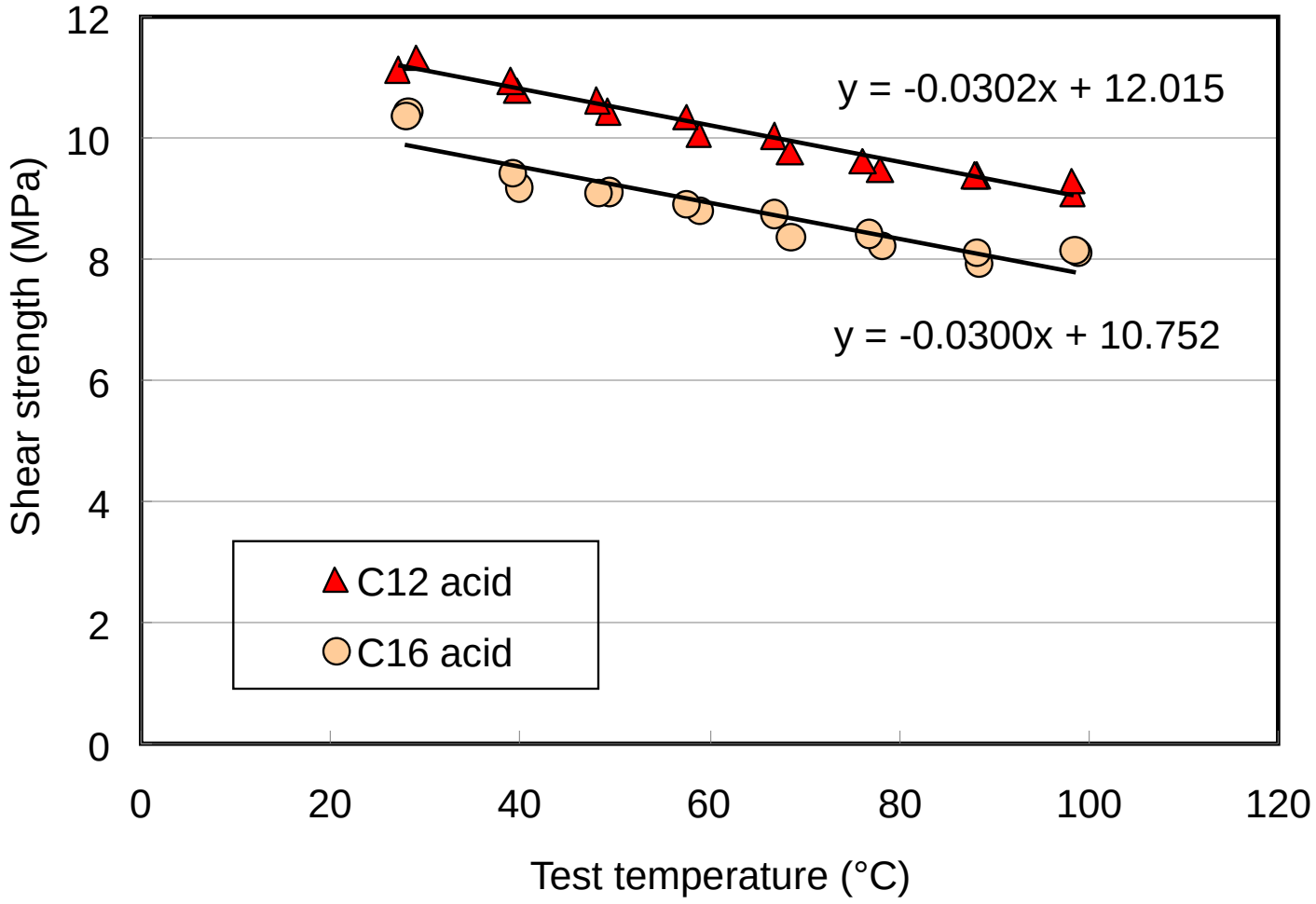

Figure 11. Variation of mean shear strength *versus* temperature for two carboxylic acid solutions at 0.01 m/s sliding speed and 3 N load.

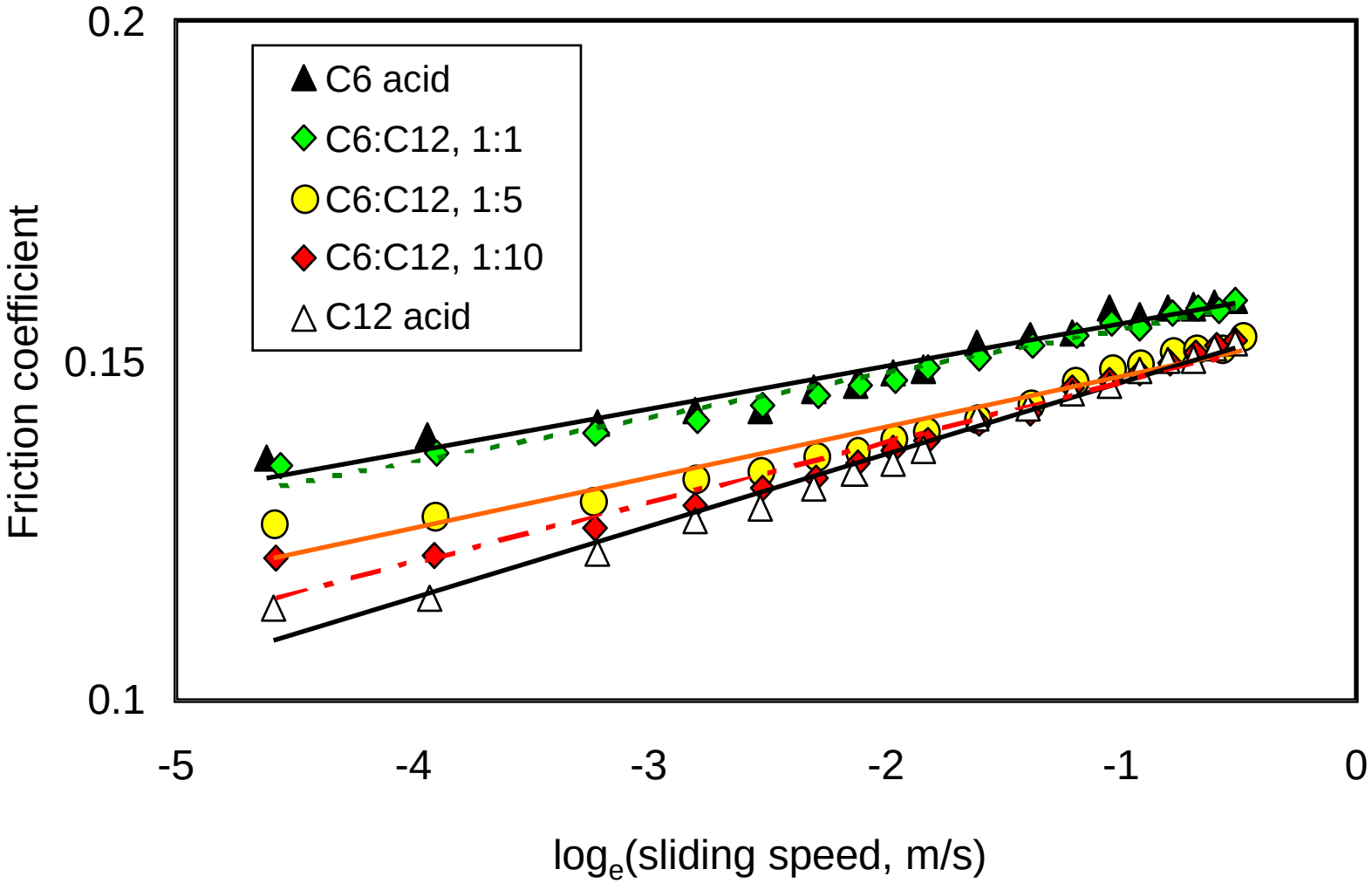

Figure 12. Linear friction coefficient *versus* logarithmic sliding speed plots for carboxylic acid blends at 100°C and 3 N load

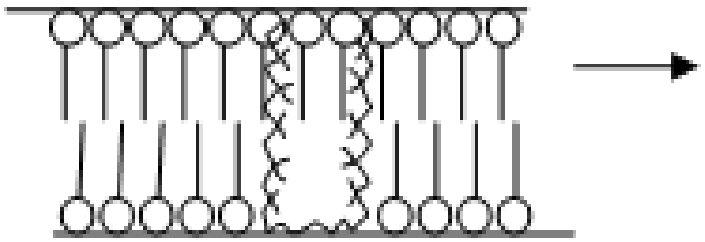

Figure 13. Schematic diagram of impact of adsorbed dispersant molecules on friction modifier film

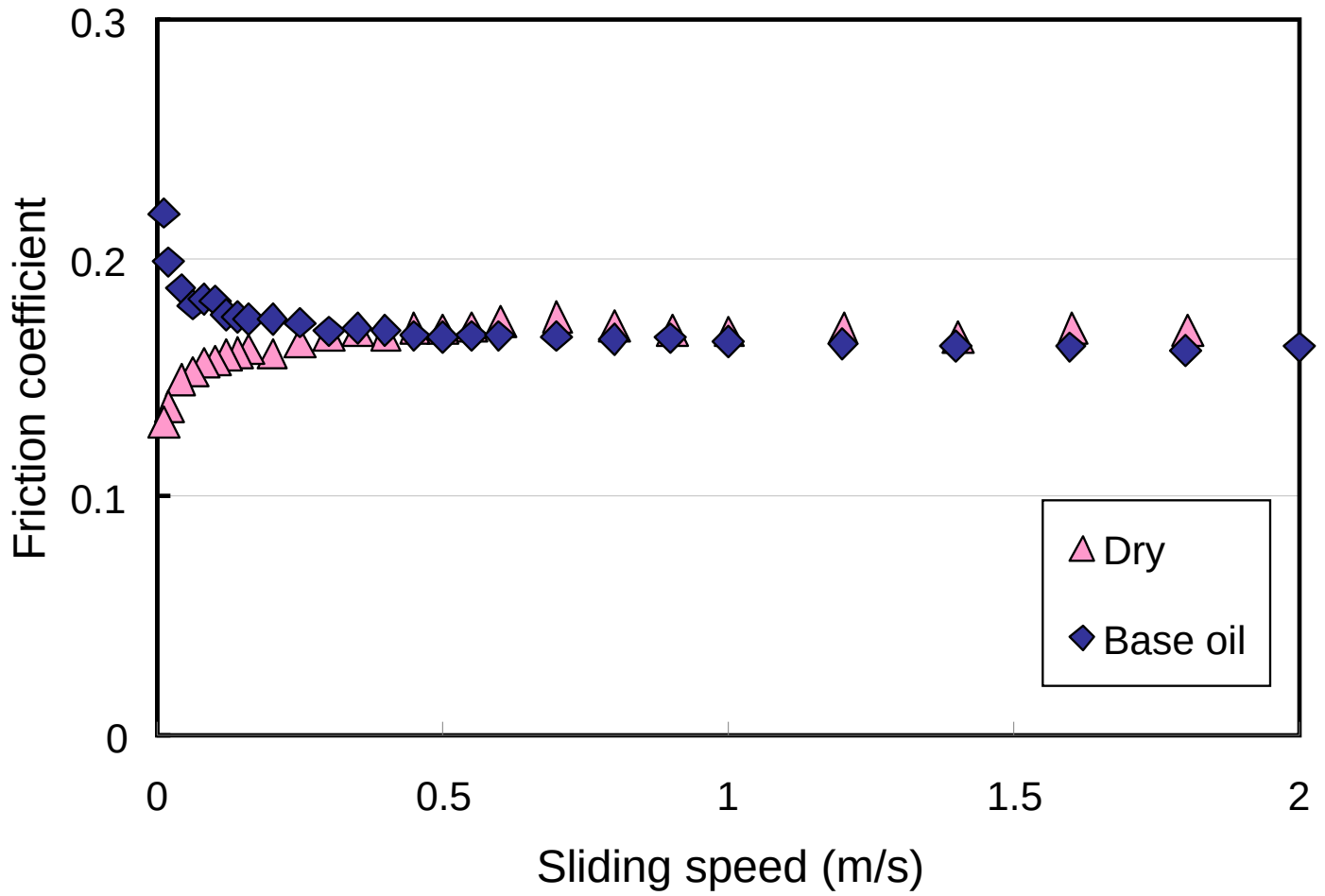

Figure 14. Friction coefficient versus sliding speed curve for sliding contact of (i) dry friction material/steel contact and (ii) base oil lubricated friction material/steel contact; (3 N load, 100 °C)

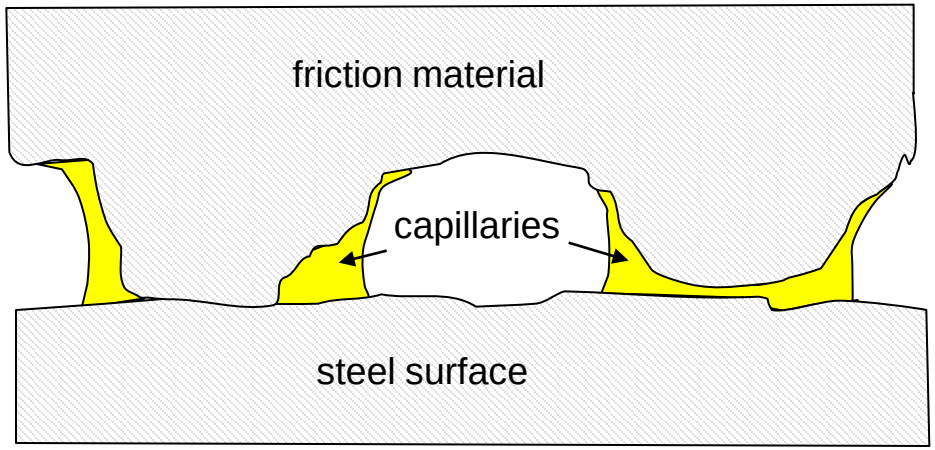

Figure 15. Schematic diagram of fluid bridging the friction material/steel surfaces due to capillary action

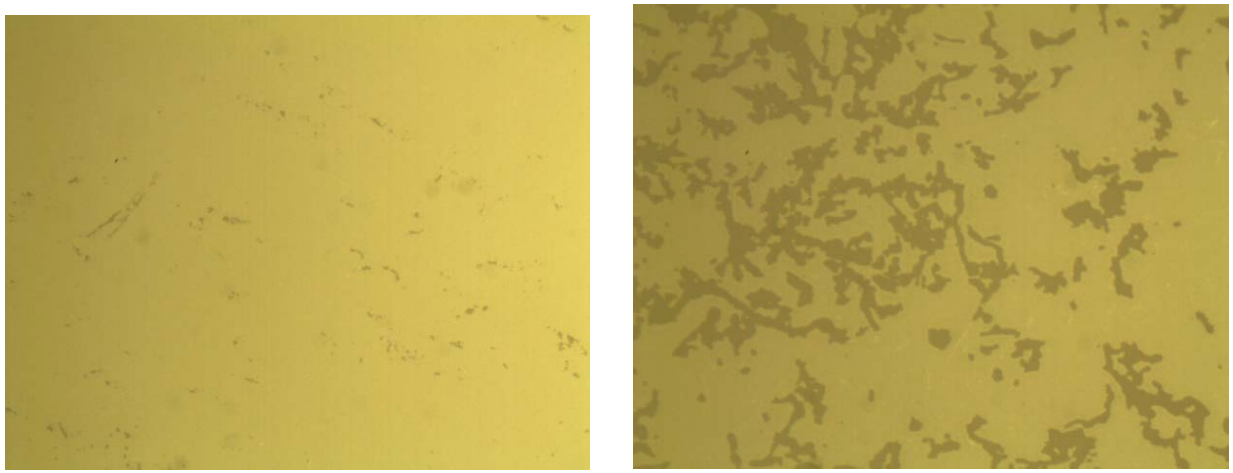

Figure 16. Optical images of contact between friction material and glass surface; (i) dry, (ii) well supplied with base oil

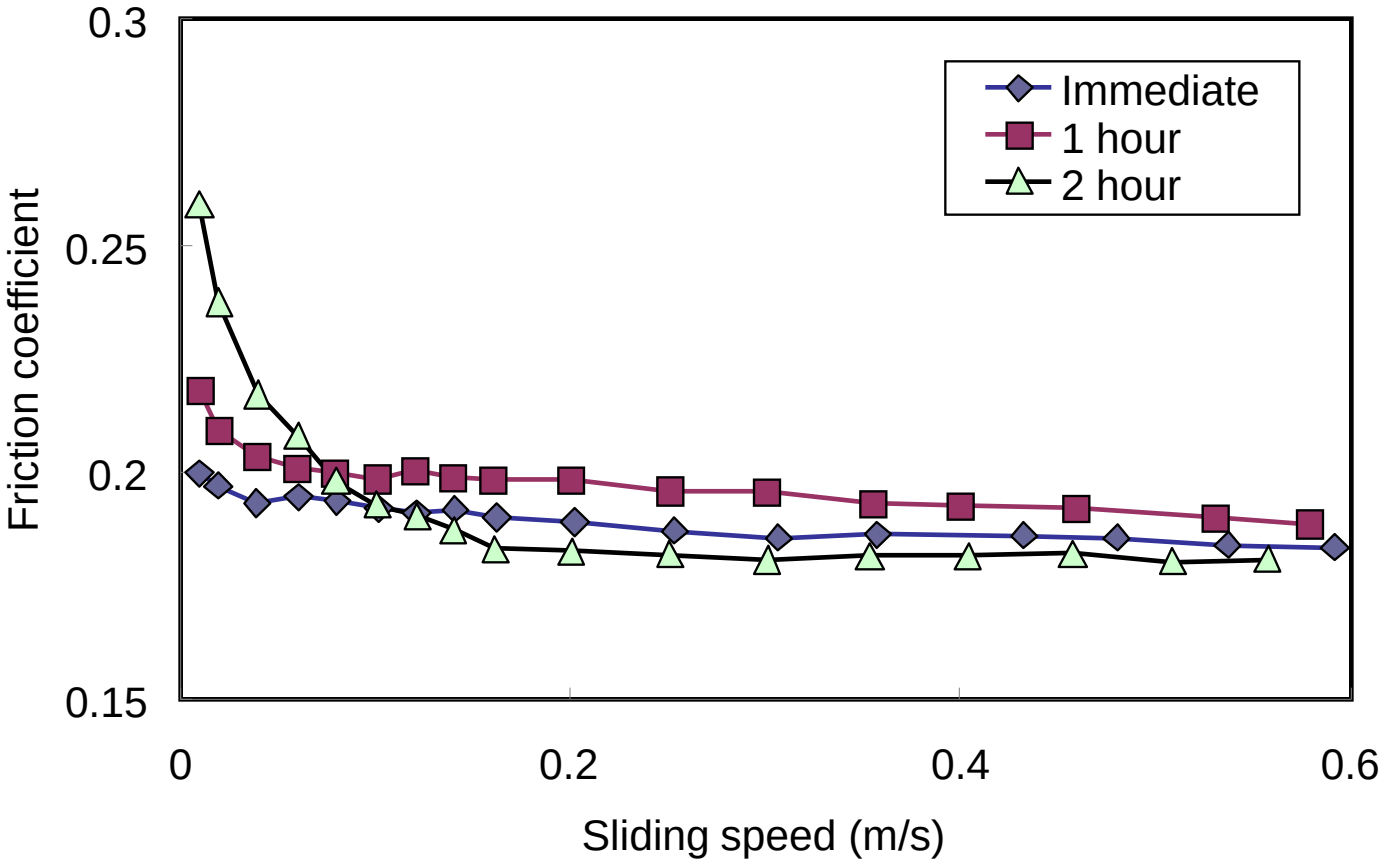

Figure 17. Friction *versus* sliding speed behaviour for base oil following plasma cleaning of friction material; (i) immediately after plasma treatment, (ii) after one hour exposure to atmosphere, (iii) after two hours exposure to atmosphere; (load = 3 N, temperature = 100°C)

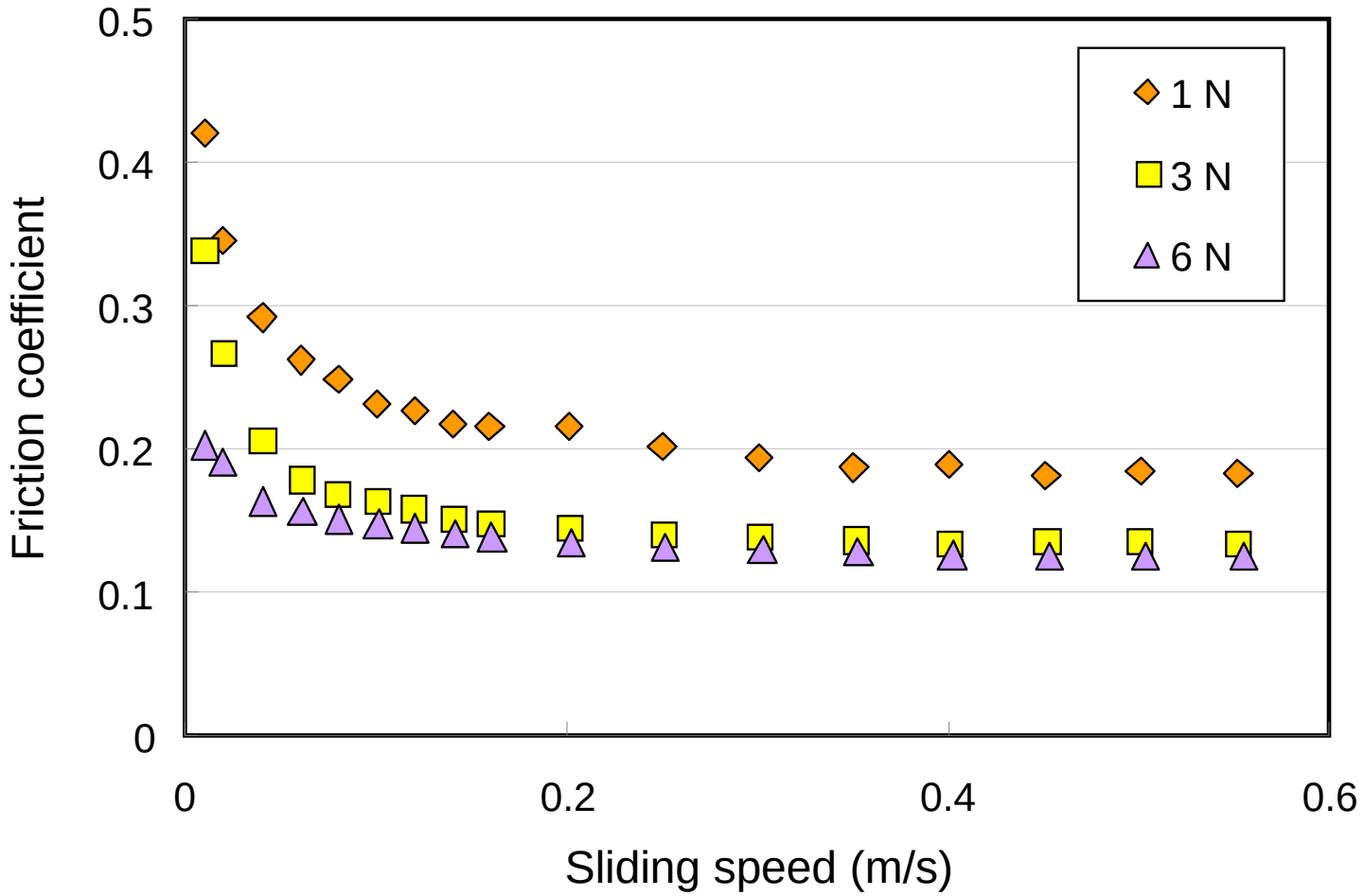

Figure 18. Friction coefficient versus sliding speed curves for hexadecane at three applied loads. Test temperature = 22°C.